Engineering Applications of Artificial Intelligence 128 (2024) 107388

Contents lists available at ScienceDirect

Engineering Applications of Artificial Intelligence

journal homepage: www.elsevier.com/locate/engappai

Seismic response and performance prediction of steel buckling-restrained braced frames using machine-learning methods

N. Asgarkhani [a,*], F. Kazemi [a,b], A. Jakubczyk-Gałczyńska [a], B. Mohebi [c], R. Jankowski [a]

[a] Faculty of Civil and Environmental Engineering, Gdańsk University of Technology, ul. Narutowicza 11/12, 80-233, Gdansk, Poland
[b] Department of Civil, Environmental & Geomatic Engineering, University College London, London, UK
[c] Faculty of Engineering and Technology, Imam Khomeini International University, Qazvin, Iran

ARTICLE INFO

Keywords:
Buckling-restrained braced frame
Machine-learning algorithm
Residual interstory drift
Seismic retrofit
Seismic performance curve
Seismic failure probability

ABSTRACT

Nowadays, Buckling-Restrained Brace Frames (BRBFs) have been used as lateral force-resisting systems for low-, to mid-rise buildings. Residual Interstory Drift (RID) of BRBFs plays a key role in deciding to retrofit buildings after seismic excitation; however, existing formulas have limitations and cannot effectively help civil engineers, e.g., FEMA P-58, which is a conservative estimation method. Therefore, there is a need to provide a comprehensive tool for estimating seismic responses of Interstory Drift (ID) and RID with novel approaches to fulfill the shortcomings of existing formulas. The Machine Learning (ML) method is an interdisciplinary approach that makes it possible to solve these types of engineering problems. Therefore, the current study proposes ML algorithms to provide a prediction model for determining the seismic response, seismic performance curve, and seismic failure probability curve of BRBFs. To train ML-based prediction models, Nonlinear Time-History Analysis (NTHA) and Incremental Dynamic Analysis (IDA) were performed on the 2-, to 12-Story BRBFs subjected to 78 far-field ground motions, and 606944 data points were prepared for different prediction purposes. The results indicate that the considered approaches are justified. For instance, the proposed ML methods have the ability to predict the maximum ID, maximum RID and maximum roof ID with the accuracy of even 98.7%, 95.2%, and 93.8%, respectively, for the 4-Story BRBF. Moreover, a general preliminary estimation tool is introduced to provide predictions based on the input parameters considered in the study.

1. Introduction

Buildings that are designed following the seismic codes can be prevented from failure during earthquakes due to excessive deformation, thereby, ensuring that residents are safe (Giugliano et al., 2010). During seismic events, the plastic deformation of structural components (i.e., beams, columns, and braces) leads to residual deformation of the building, known as Residual Interstory Drift (RID). The ratio of RID plays a significant role in deciding between repairing buildings after seismic excitation and the cost of retrofitting (Yahyazadeh and Yakhchalian, 2020). Following the 2011 Christchurch earthquake, it is evident that repairing buildings with large RID is extremely difficult, and most of the buildings should be demolished due to the high cost of retrofitting (Cole et al., 2012). According to the study conducted by McCormick et al. (2008), reconstructing is more cost-effective than repairing buildings having a maximum RID larger than 0.5%. Hence, owing to its importance, some researchers assessed this characteristic of the buildings and proposed a formula to estimate the RID for some types of structures. Estimating RID can facilitate the process of design and analysis while improving the knowledge of engineers about the current state of the building. Different formulas have been proposed so far to evaluate the RID of buildings. For instance, Ruiz-García and Miranda (Ruiz-Garcia and Miranda, 2010) conducted a probabilistic approach to predict the RID demands of multi-story buildings approximately in seismic evaluation. They showed that there is a relationship between the maximum Interstory Drift (ID) and RID based on the mean annual frequency of exceedance and the number of floor levels. Moreover, there is a formula defined in FEMA P-58 (FEMA P-58, 2012) that can be used to calculate the median RID of different stories in a building. Although a building can experience unpredicted values of RID during seismic events, it is possible to increase the performance of the building by improving its capabilities, such as enhancing the beam-to-column connections, using outer frame infills to resist lateral deformations, and implementing viscous dampers as dissipative devices. While there is still

* Corresponding author. Faculty of Civil and Environmental Engineering, Gdańsk University of Technology, ul. Narutowicza 11/12, 80-233 Gdansk, Poland.
E-mail address: neda.asgarkhani@pg.edu.pl (N. Asgarkhani).

https://doi.org/10.1016/j.engappai.2023.107388
Received 27 April 2023; Received in revised form 3 October 2023; Accepted 26 October 2023

a need to provide a comprehensive tool for estimating seismic responses of ID and RID, existing formulas have limitations and cannot effectively help civil engineers. Therefore, this study investigates novel approaches to fulfill the shortcomings of existing formulas.

The Buckling-Restrained Brace (BRB) is a kind of bracing system with the capability of good energy dissipation through stable hysteretic cycles in both tension and compression. As an alternative to steel Moment Resisting Frames (MRFs) and concentric braced frames, BRBs can be able to overcome the limitations of both of them, providing the structural system with adequate stiffness and ductility (Jia et al., 2017; Xie et al., 2020). This system consists of a central steel core surrounded by steel tubes filled with concrete. This prevents the core from buckling and the brace is capable of yielding in tension as well as in compression (Barbagallo et al., 2019). The main concern of this system is the low post-yield stiffness of the core that leads to a large RID after the occurrence of an earthquake and a higher weight of the device (Sabelli et al., 2003; Erochko et al., 2011). Therefore, several studies have been focused on evaluating the RID of structures equipped with BRBs. To reduce the amount of RID in these systems, some researchers used shape memory alloys (Ghowsi and Sahoo, 2020), and others implemented it as dual-frame lateral resistance (Maley et al., 2010; Deylami and Mahdavipour, 2016; Baiguera et al., 2016; Montuori et al., 2016). Xie et al. (2020) assessed the hysteretic performance of self-centering BRBs using friction fuses empirically and showed that reducing the RID by implementing the friction fuses is possible.

Recent studies confirm that the modeling process, design and analysis of Buckling-Restrained Brace Frames (BRBFs) may impose an additional cost while predicting the seismic responses such as ID and RID can help civil engineers to find out the current performance of the BRBFs, reducing the time of modeling, and provides a preliminary estimation. To do this, some researchers tried to estimate the RID of BRBFs by proposing some formulas. Erochko et al. (2011) evaluated the RID of BRBFs and steel MRFs, and then, introduced a formula for predicting the mean RID of different stories of these systems. Ruiz-García and Chora (2015) designed three-, and thirteen-story steel MRFs to estimate RID demands using FEMA P-58 (FEMA P-58, 2012) and Erochko et al. (2011) methods. Finally, they introduced a procedure, named the coefficients method, for predicting the RID of steel MRFs. Asgarkhani et al. (2020) evaluated the approximate methods to predict the RID of BRBFs considering the effects of strain hardening ratio in different ground motion intensity-levels. To estimate the median RID of BRBFs, they proposed a new method based on the analysis results. Yakhchalian et al., 2020, 2021 investigated the efficiency and sufficiency of some traditional and advanced intensity measures for predicting the maximum RID capacity of BRBFs.

Recently, earthquake engineering has begun to implement emerging soft computing techniques, such as Machine Learning (ML) models, and the use of these techniques is expected to expand in this field over the coming years (Shafighfard et al., 2022; Zhang and Burton, 2019). A range of methods for seismic response estimation in buildings is envisioned, spanning from fundamental mechanics-based approaches to purely data-driven ML models. Mechanics-based approaches rely on engineering principles, while data-driven models utilize parametric datasets from nonlinear analyses. To summarize the recent works related to seismic response assessment of BRBFs, Table 1 has been provided (Gholami et al., 2021; Sun et al., 2020; Jagruthi et al., 2022; Tamimi et al., 2023; Asgarkhani et al., 2023) (see Table A-1 in *Appendix* that presents the abbreviations and acronyms list used in this research). It can be seen that while most contributions only focused on the ID and RID, this study aims to provide a wide range of seismic responses and performance curves that can be used for retrofitting buildings. The results of predictions can be used to evaluate the current performance of the building, and then, it would be possible to evaluate the economical aspect, possibility of retrofitting, and cost of retrofitting based on the performance curve. Moreover, the literature review showed that previous studies relied on the conventional ML algorithms, while in this research the Stacked model is proposed.

Table 1
Summarized literature review related to seismic response estimation of buildings.

Ref.	Structure	Response evaluation	Modeling	Description
Erochko et al. (2011)	BRBFs and MRFs	RID	Numerical models of 2-, 12-story BRBFs and MRFs	Introduced a formula for estimating the RID of the structures
Ruiz-García and Chora (2015)	MRFs	RID	Numerical models of 3-, 13-story MRFs	Introduced a formula based on the maximum drift, elastic drift, and the drift concentration factor
Asgarkhani et al. (2020)	BRBFs	RID, coefficient of distortion for RID	Numerical models of 2-, 12-story BRBFs	Proposed method is more accurate than the FEMA P-58 (FEMA P-58, 2012) and Erochko et al. (Erochko et al., 2011) methods
Gholami et al. (2021)	BRBFs	RID	ABAQUS software model for 6-story BRBF	Adding post-tensioned frame to control RID of BRBFs
Sun et al. (2020)	BRBF	ID	48-story building was modeled	ANNs was used to estimate ID of building.
Jagruthi et al. (2022)	BRBF	ID	8-story building was modeled in OpenSees	KNN, DT, RF, AdaBoost, XGBoost, LightGBM, and CatBoost algorithms have been used
Tamimi et al. (2023)	BRB	Reliability assessment of gap size	12000 samples of BRB	ANNs and Monte Carlo simulations have been used
Asgarkhani et al. (2023)	MRFs	ID, RID, seismic risk assessment	1034976 data points from 2-, to 9-story buildings	32 ML algorithms have been used for estimating seismic response of 384 MRFs

In this research, ML-based prediction models are introduced with the capability of estimating the maximum ID and RID of BRBFs, the distribution of ID and RID at floor levels of BRBFs, and the number of floor level with maximum ID and RID, which can be used to effectively estimate the behavior of BRBFs and recognizing the weak floor level. This can be considered as a preliminary evaluation of buildings that can help designers for retrofitting of buildings. Moreover, this study aims to provide a wide range of seismic evaluations, such as seismic performance curves, which can determine the seismic performance levels, and seismic failure probability, which can be used for seismic risk assessment of BRBFs. In addition, the preliminary tool has been introduced to easily modify and improve BRBFs without additional computational analysis, which significantly decreases the time of analysis. It should be noted that this tool could be updated since it uses a database and future capabilities will be added. This research includes six sections, in which the first section explains the literature reviews and the research gap in existing studies. The second section has been devoted to the modeling of BRBFs and procedures used for preparing numerical models, and the third section explains the nonlinear analysis used in this study. The ML methods used in this research, results, and discussions are explained in section four, and the general use of the proposed ML-based model is described in section five.

The innovation and operational success of this work are centered on

the development of a sophisticated Graphical User Interface (GUI) that significantly enhances seismic performance assessments for BRBFs. This innovation transcends traditional formulas and approaches, providing a forward-thinking solution to prevalent challenges in seismic engineering. In terms of innovation, the GUI incorporates ML-based prediction models, a ground-breaking approach that revolutionizes seismic response estimation. By leveraging ML, the interface can predict various seismic responses of BRBFs accurately, allowing civil engineers to assess buildings swiftly and efficiently. This departure from conventional methods marks a paradigm shift, displaying the adaptability and modernization of seismic analysis.

The operational success of the GUI lies in its practical utility and user-friendly design. Civil engineers can effortlessly navigate the interface, input relevant parameters, and swiftly obtain essential seismic response predictions. The tool's efficiency in handling diverse input parameters and generating reliable predictions in real-time significantly streamlines the design and analysis process. Engineers can readily access crucial data and insights to make informed decisions, expediting building design or retrofitting projects.

To optimize operational success further, the GUI's adaptability and future-proofing mechanisms come into play. The ability to use a database and the potential for future updates to overcome limitations underscore the forward-thinking nature of this tool. Engineers can continually improve and expand the GUI's capabilities to accommodate evolving building specifications, ensuring its relevance and effectiveness in the ever-changing field of seismic engineering.

2. Modeling methods

In this study, two groups of buildings with floor levels of 2-, to 12-Story were designed, which the first group has five spans with a length of 7.32 m and the second group has four bays with a length of 9.14 m in X direction. The outer frame of buddings is equipped with BRBF as the lateral-resisting system and other frames designed for gravity loads. All connections were assumed as pin connections; then, each BRBF should be able to resist the proper loads of floor levels divided equally between outer systems. Fig. 1 presents the regular plan of the two assumed groups with the tributary load area of BRBFs that are shown with shaded parts in the figure.

The floor height in all structures was considered equal to 3.96 m. Buildings were located in California with a latitude of 37.88° N and a longitude of 122.08° W, which soil D is considered for them following ASCE 7–16 (ASCE/SEI 7-16, 2017). Therefore, the values of spectral acceleration for the considered design site (i.e., SD_S and SD_1) can be determined as 1.25 g and 0.60 g, respectively. It is noteworthy that gravity loads in GCR 10-917-8 report (GCR 10-917-8, 2010) were selected for designing the buildings using ETABS 2016 software. Fig. 2 illustrates the 3D view of the 6-Story building modeled in ETABS 2016 software. To determine lateral loads, the equivalent lateral load manner was utilized according to AISC 360-16 (ANSI/AISC 360–16, 2016) and AISC 341-16 (AISC 341-16, 2016) considering the values of R = 8.0 and I = 1.0, respectively. Given that, the plan of buildings is regular, the models include one bay of the four bays (i.e., building with four bays in X direction) and five bays (i.e., building with five bays in X direction) that were modeled by OpenSees (McKenna et al., 2015) for conducting nonlinear analyses. It should be noted that the details of structural elements of braced spans were obtained from ETABS 2018 software to be used for 2D modeling, which is presented in Figs. A-1 and A-2 in *Appendix*.

Fig. 3 illustrates the considered modeling method of the BRBF in OpenSees (McKenna et al., 2015). The yielding segment of each brace (i.e., brace core) was assumed 0.7 times the length of the work point-to-work point of the brace, which is defined based on the central nodes of structural elements depicted in Fig. 3. A beam-column element having five integration points was used for modelling beams, columns, and brace cores. A fiber section based on the Giuffre-Menegotto-Pinto model was defined for each element using *Steel02* material (Mazzoni et al., 2006). Beams and columns were assumed to have a yield stress of 379.2 MPa, while this value for the brace cores was considered 289.6 MPa. The structural members were assumed to have an elastic modulus of 200 GPa. Different values of strain hardening ratio, α, have a great influence on the residual deformation of BFBFs; therefore, strain hardening ratios of 0.003, 0.01, and 0.02 were used for modeling 2D models (Asgarkhani et al., 2020; Yakhchalian et al., 2020, 2021). Guerrero et al. (2016) proposed values for the parameters of *Steel02* that can be applied to monitor the material transition from plastic to elastic states and its hysteretic response. This transition is controlled by parameters of R0, CR_1 and CR_2 having values of 20.0, 0.925, and 0.15, respectively. Additionally, the default values for the isotropic hardening parameters of *Steel02* material for columns and beams were $a_1 = 0.0$, $a_2 = 1.0$, $a_3 = 0.0$, and $a_4 = 1.0$. Assuming the higher strength of BRBs in the compression compared to the tension, Guerrero et al. (2016) performed a calibration for $a_1 = 0.07$ and $a_3 = 0.05$ parameters of the *Steel02* material (see more detail (Asgarkhani et al., 2020)). The verification of the behavior of BRB element and the procedure used for modeling was conducted by Asgarkhani et al. (2020). Moreover, the other gravity column effects were modeled as a leaning column to take into account the P-Δ effects (Asgarkhani et al., 2020; Yakhchalian et al., 2020, 2021).

3. Nonlinear analysis

In this research, two nonlinear dynamic analyses of Nonlinear Time-

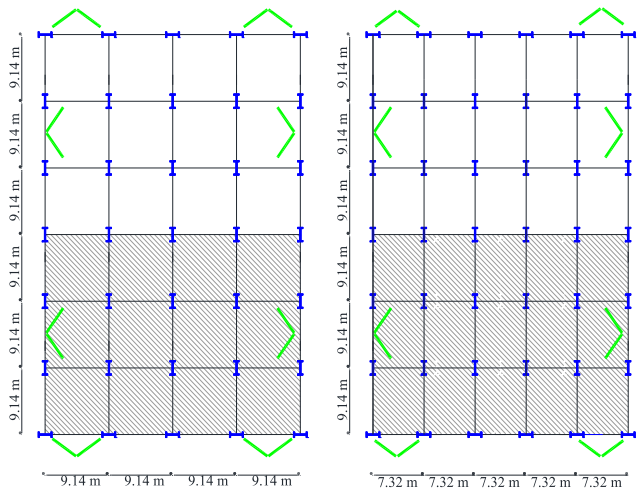

Fig. 1. Two regular plans used for modeling of BRBFs.

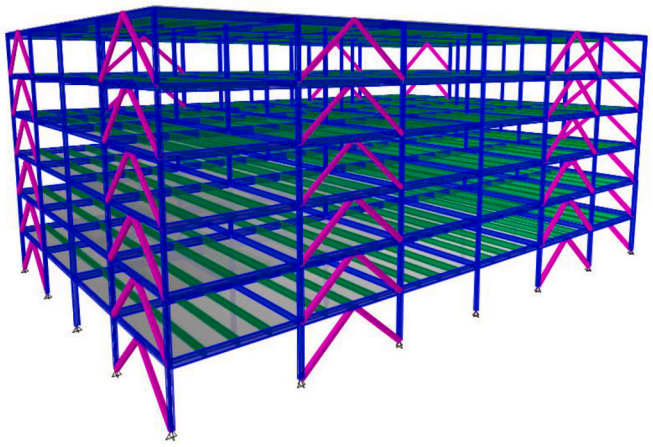

Fig. 2. The 3D view of the 6-Story building modeled in ETABS 2016 software.

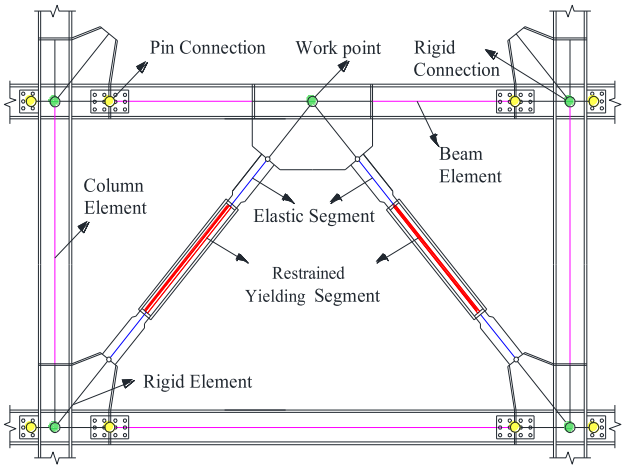

Fig. 3. Considered modeling method of the BRBF in OpenSees (McKenna et al., 2015) software.

History Analysis (NTHA) and Incremental Dynamic Analysis (IDA) were performed to achieve the seismic response of ID, RID, seismic performance, and seismic failure probability of BRBFs. The procedure used for the analysis and the results of each analysis are discussed in the following subsections.

3.1. Nonlinear time-history analysis

In the NTHA, each seismic record is applied to BRBFs with a specific scale factor. To have a reference for comparison of the responses, a procedure is introduced for achieving the scale factor of the analysis. In this research, seven intensity levels of $R = 1.25$, 1.5, 2.0, 3.0, 4.0, 5.0, and 6.0 were considered, which could be determined as follows:

$$R = \frac{S_a(T_1)}{\gamma}, \gamma = \frac{V_y}{W_{Seismic}} \tag{1}$$

where $S_a(T_1)$ known as the spectral acceleration at the first period of BRBF, and V_y and $W_{Seismic}$ are determined by base shear at the first yielding point of the pushover curve and seismic weight of BRBF, respectively. Since the V_y is determined in the first yielding point of the pushover curve, the values of V_y do not depend on α value. Therefore, in each value of R, a scaled seismic record should have the same spectral acceleration at the first period $S_a(T_1) = R \times \gamma$. In this research, all assumed BRBFs were analyzed based on the assumed values of R, and 78 seismic ground motions. Then, the results of RID and ID in each story level and top floor level, and the story number of the maximum values of RID and ID were determined to be defined as data points for the ML algorithms.

3.2. Incremental dynamic analysis

The IDA is a well-known analysis for estimating the performance curve of the structure that can be used for seismic performance level assessment. This analysis includes some NTHA with increasing the intensity of the ground motion records (i.e., $S_a(T_1)$) until reaching the total

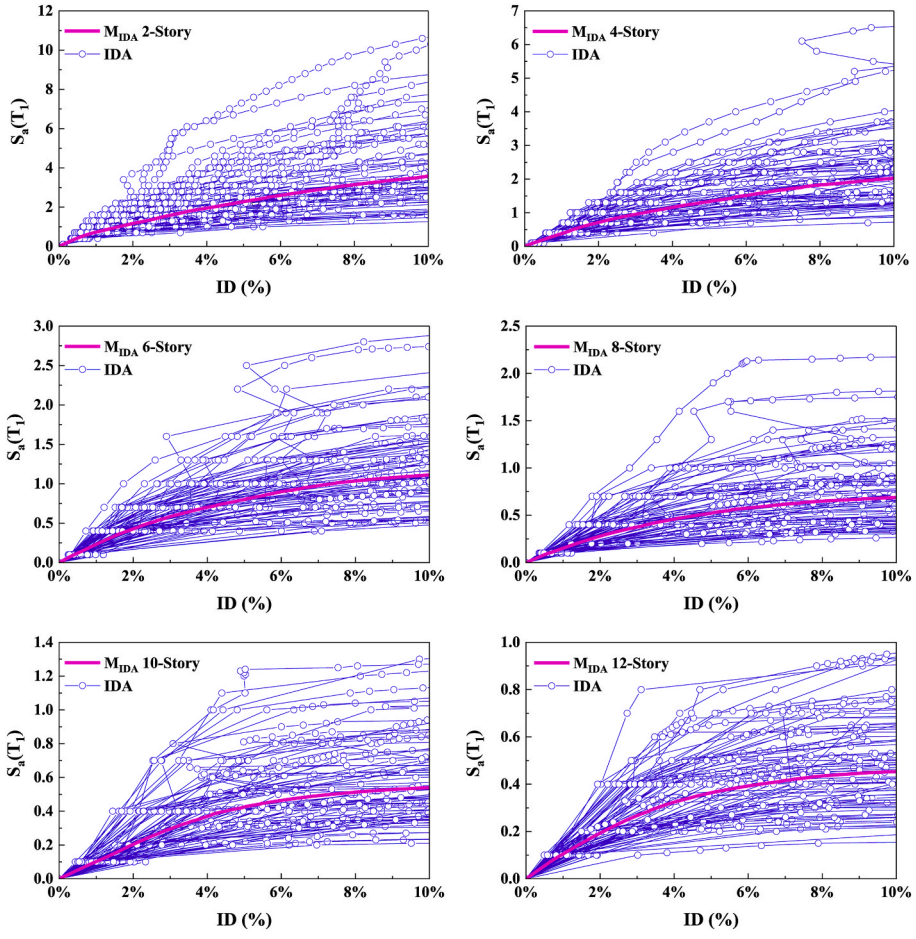

Fig. 4. IDA curves of 2-, to 12-Story BRBFs with the bay length of 7.32 m and strain hardening ratio of 0.003.

collapse of the structure. Due to the importance of this curve, there is a need to provide a big computational effort for analysis; therefore, the hunt & fill method was used, which can reduce the time of analysis (Haselton, 2006; Kazemi et al., 2023a). Since the constructional site of buildings was classified as far-field site, a set of 78 far-field ground motions was considered according to Haselton (Haselton and Deierlein, 2007). Fig. 4 illustrates the IDA curves of BRBFs with a bay length of 7.32 m and strain hardening ratio of 0.003.

4. Machine learning methods

Recently, a growing number of disciplines have employed artificial intelligence techniques for predicting processes in a variety of fields. The ML is a subset of artificial intelligence, which identifies patterns in data to predict or classify them. In comparison to conventional approaches, ML methods are considered a powerful tool for solving complex problems, with the ability to facilitate the process of making decisions by improving computational efficiency and propagating uncertainties and treating them. Nowadays, ML methods are widely used by researchers to provide a prediction model that can be employed to facilitate the estimation of structural responses and optimization problems (Panagant et al., 2021). According to the literature review, Artificial Neural Networks (ANNs) have the ability to train and learn during the process that has been conducted in two main procedures of feed-forward and feed-backward propagation, which can be used for reliability analysis and optimization problems (Meng et al., 2023). Using this procedure helps the method to be rectified during the training and improves the prediction accuracy. In feed-forward propagation, the input features are defined and activation functions between the hidden layers are determined to finally achieve the output. Differences between the actual value of output and the predicted one, which is known as the error value, cause the algorithm to be rectified using feed-backward propagation. This loop can be repeated many times to achieve the best prediction value with the lowest error value. Fig. 5 illustrates the architecture of the feed-forward and backward propagation method in ANNs (Oh et al., 2020; Kazemi et al., 2023b).

Recurrent Neural Networks (RNNs) are a type of neural network architecture designed to process sequential and temporal data. Unlike traditional feed-forward ANNs, the RNNs have connections between nodes form directed cycles for allowing them to retain and utilize information from previous time steps. This recurrent connection allows the network to capture dependencies and patterns across time, making RNNs particularly effective for tasks involving sequential data, such as time series analysis. Unlike RNNs, ANNs do not have cyclic connections and process input data independently without considering temporal relationships. ANNs are effective for tasks where the order of the input does not matter or is irrelevant.

Although the decision tree algorithm has the ability to divide the tree according to thresholds, using the Random Forest (RF) method with regulation parameters can improve the accuracy and speed of calculations. The RF method can employ a forest for specific training data that spreads the decision trees for each part of the training data, and finally, it cumulates the prediction results of all decision trees using randomly selected subsets of the main dataset. The Extra-Trees Regressor (ETR) is a developed version of the RF method that selects a random threshold in each tree. The Bagging Regressor (BR) is another improved algorithm that has the ability to fit the predicted value in each random subset and aggregates the result based on the individual predictions (see more details (Kazemi et al., 2023b; Kiani et al., 2019; Todorov and Billah, 2022)).

Boosting methods have become the mainstream of ML algorithms since they have the ability to improve weak learners into strong learners using a combination of models. Boosting algorithms can be categorized into five methods, namely, Gradient Boosting Machine (GBM), Adaptive Boosting (AdaBoost), Extreme Gradient Boosting (XGBoost), Light GBM, and CatBoost. The GBM employs a primary predictive model to estimate the output, then, uses the second predictive model for improving the prediction values and reducing the error. This procedure is continued to find the best-fitted model. The Histogram-based Gradient Boosting Regression (HGBR) uses the quantization procedure to split the features and improves the speed of calculations compared to the GBM. The AdaBoost method uses a combination of strong base learners to create a prediction model based on the weight of data (Shafighfard et al., 2022; Kazemi and Jankowski, 2023; Kazemi et al., 2023c).

To reduce the overfitting or underfitting issues of the GBM, various regularization methods have been used by the XGBoost algorithm that enhances the performance of the predictive model while increasing the speed of calculations. Fig. 6 illustrates the visual representation of the XGBoost and LightGBM algorithms. The LightGBM method can be used for big data points while it performs with higher efficiency and calculation speed. It is noteworthy that the LightGBM uses leaf-wise tree growth instead of level-wise tree growth, which is implemented by the XGBoost algorithm. Since the classical boosting algorithms are prone to overfitting or underfitting issues, the CatBoost method employs a permutation-driven approach for training the model while residuals are determined on another subset to prevent data leakage. Although many ML algorithms can be used for a regression problem, in this study, the previously introduced methods were used to propose a multi-functional prediction model (for more detail regarding the ML algorithms see (Kazemi et al., 2023b; Kazemi et al., 2023c)). It should be noted that a dataset containing 606944 data points was prepared from analysis to be used in the prediction models. The test data points have been varied due to the type of output. In other words, when it comes to predicting the seismic responses of the 4-Story BRBF, all the results related to the 4-Story BRBF have been removed from the training dataset to prevent data leakage; then, the prediction models have been used to estimate the outputs of the selected structure. Therefore, in each type of output, there are different numbers of data points in the training and testing dataset. In addition, the same procedures have been done in the curve plot ability

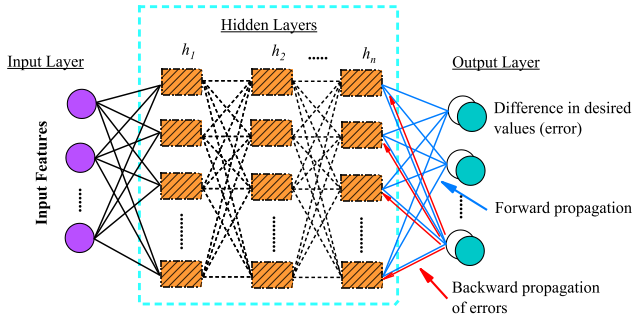

Fig. 5. The architecture of the feed-forward and backward propagation method in ANNs.

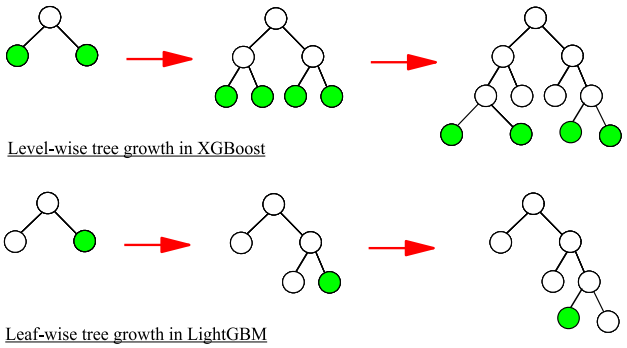

Fig. 6. Visual representation of the XGBoost and LightGBM algorithms.

of the ML models for estimating seismic performance and failure probability curves. The term "seismic responses" can be defined as a response of structure during seismic load, e.g., earthquake, in which this response can be determined by monitoring the behavior of structural elements and floor levels. This research comprehensively investigates different seismic responses of distribution of RID and ID at each floor level, RID and ID at the top floor level, the story number of the maximum values of RID and ID, the median of IDA curves, and the seismic failure probability curve.

4.1. Partial dependence plot

The relative importance of input features can present the importance of each feature on the predicted response of BRBFs. Therefore, it would be possible to ignore the feature having lower importance. To find out the negative or positive effects of features on the prediction target, the Partial Dependence Plot (PDP) that was introduced by Friedman (2001) presents the expected effects of each feature on the output of ML-based prediction models using a marginalizing process of all input features and plotting the outcomes of a prediction model based on the input feature (Feng et al., 2021). Since many factors can affect the seismic response of BRBFs, in this research, all of the structural factors have been considered; then, the PDP of input features used in the XGBoost algorithm have been plotted to find out the relevance of the features. Although there is more than one output for prediction, the PDP of the distribution of ID has been illustrated in Fig. 7 as an example.

Fig. 7 presents the PDP of input features used in the XGBoost algorithm compared with the variation of the input features for estimating the distribution of ID. According to these plots, the thresholds in which the prediction model is varied corresponding to the variation of input features are provided to show the influence of each feature on the estimation of seismic response of BRBFs. It can be observed that increasing the weight, number of stories, and building height can lead to a small increase in the prediction of seismic responses; while the increase in RSN shows a fluctuated increase and decrease in the values of prediction that confirms the dependence of the results to the ground motion records used for the analysis. In addition, the increase in base shear, T_1 and R_y lead to an increase in the prediction of seismic responses, although the effect of R_y is more evident compared to others. In addition, γ and α have vice versa effects, in which by increasing the values of γ and α, their effects are reduced correspondingly. The results confirm that the modeling parameters introduced as input features considerably affect the estimation of the seismic response of BRBFs. According to the results of Fig. 7, ten input features have been selected that have the highest effects on the results of the analysis. It should be noted that due to the constant influence of other features, they are removed from comparison and do not consider as input features of ML models.

4.2. Proposed stacked ML

Previous studies confirmed that there is no unique ML algorithm for estimating the seismic response of structures since the nature of the seismic event and the response of the structure to this external load is unpredictable. In this study, one of the most important goals is to propose an ML-based prediction model that can provide the estimation of seismic responses with the minimum number of training data points. This ability can help future studies to easily provide the training dataset of ML algorithms. Previous investigations of authors showed that some ML methods have the capability of predicting the seismic responses, while still there is a need to improve their performances. In this study, the Stacked ML model is introduced to cover the shortcomings. Using all ML methods in combination with one algorithm, such as ensemble ML or Stacked ML algorithms, increases the time of predictions. Therefore, the

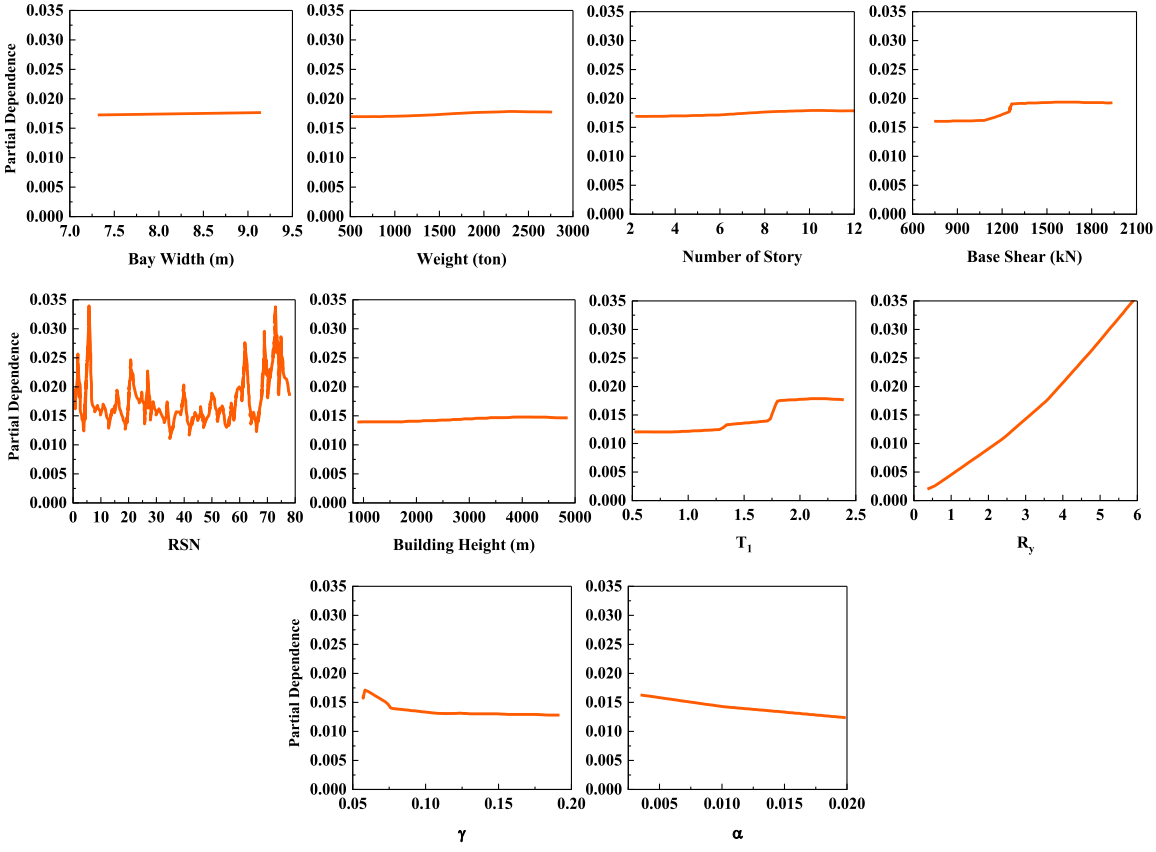

Fig. 7. Partial dependence plot of input features used in the XGBoost algorithm.

proposed Stacked ML algorithm should be a well-organized method for the training dataset to ensure that it can work with different features of data points.

The proposed Stacked ML algorithm includes the feature selection methods (i.e., filter, wrapper, and embedded methods) that are used to omit the redundant input features from the dataset. In addition, the hyperparameters are optimized based on the optimization algorithm embedded in the Tree-based Pipeline Optimization Tool (TPOT) as an AutoML method in Python software (i.e., Auto-sklearn). Fig. 8 illustrates the automated TPOT, in which the highlighted section is done automatically. Using TPOT can improve the solutions for optimizing the ML pipelines that are used in the proposed Stacked ML algorithm. Thus, the proposed Stacked ML algorithm is tested on the prepared dataset and the best sub-models are indicated in Table 2. It should be noted that the sub-models used for the Stacked ML algorithm are optimized based on the improvements in the results and decrease the time of calculations, while the proposed algorithm can predict different seismic responses of the maximum of ID and RID in each BRBF, roof ID, the story number of maximum ID and RID, and distribution of ID and RID. In addition, the ANNs with three hidden layers having activation function of Relu is used assuming Adam as optimizer.

Since employing all of the sub-models in one model cannot fulfill the reduction of the time of calculations, a procedure is used for selecting the best combination of the sub-models used in the Stacked ML algorithm. To check the capability of the proposed ML models, first, the best hyperparameters for the prediction of ML models have been selected (see Table 2), and then, ML models have been employed in the Stacked ML model using their best hyperparameters to check the capability of them in combination model. By pre-processing the combination of one to six sub-models using the error indicators presented in Table 3, the Stacked ML algorithm, including the three sub-models of the ETR, BR, and LightGBM, has the best results and execution speed for predicting the distribution of ID and RID. Results of error indicators for the pre-processing dataset assuming proposed ML models are presented in Table 4, which shows the values of indicators for each algorithm. In the following subsections, the results of the analysis are described in detail. Moreover, the models of RF, BR, ETR, ANNs, RNNs, GBM, and XGBoost can be considered as prediction models to estimate seismic responses of the maximum of ID and RID in each BRBF, roof ID, and the story number of maximum ID and RID, as well as, the seismic performance and seismic failure probability curves.

4.3. Seismic response prediction

After investigation on the influence of input features, they are introduced as input variables for the ML algorithms and the training of the prediction models is conducted using data selection techniques such as cross-validation, filter method (e.g., Chi-square), wrapper method (e.g., forward and backward feature selection), embedded method (e.g., LASSO Regularization). To prepare a condition for comparing the ML models, a PC having the hardware details of Cori3-8100, CPU 3.60 GHz with 16 GB internal RAM has been used to execute the algorithms. All methods have been embedded in Python software and the best results of each ML algorithm have been selected and presented. Fig. 9 illustrates

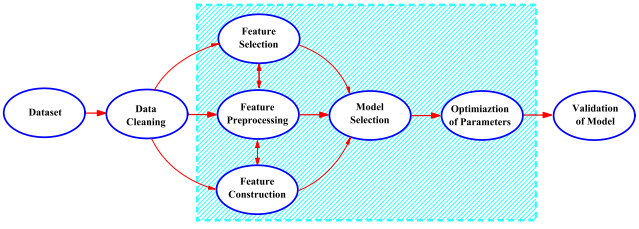

Fig. 8. Automated tree-based pipeline optimization tool.

the response predictions of the 4-Story BRBF with $\alpha = 0.003$, $R = 4$ and the bay length of 9.14 m using the ETR algorithm. It can be seen that the ETR algorithm can predict the maximum ID, maximum RID and maximum roof ID with accuracy of 98.7%, 95.2%, and 93.8%, respectively, which are higher than other ML-based prediction models used in this research. In addition, the prediction model has the ability to predict the floor level of maximum ID and RID with less error. Fig. 10 illustrates the response predictions of the 8-Story BRBF with $\alpha = 0.01$, $R = 3$ and the bay length of 7.32 m using the ETR algorithm, which the ETR algorithm predicted the maximum ID, maximum RID and maximum roof RD with the accuracy of 91.2%, 96.7%, and 92.4%, respectively, that confirms the ability of proposed models.

The Leave-one-out Error (LE) is a technique for estimating the model's performance by leaving out one data point at a time from the training set and evaluating the model's prediction on the omitted data point. This process is repeated for each data point in the dataset. The LE provides an estimate of the model's generalization performance, assessing its ability to make accurate predictions on unseen data. To better compare the performance of ML models, the LE is determined for the response predictions of the 4-, and 8-Story BRBFs presented in Figs. 9 and 10. The results confirmed the capability of the ML model used for estimating the seismic responses.

Although the ETR algorithm shows the best predictions of maximum ID, RID, and roof ID, in some cases, the LightGBM, ANNs, and XGBoost have better performances. For estimating the distribution of ID along the floor levels of BRBFs, it is not possible to select the best algorithm, since different methods have determined the accurate values at each floor level. Therefore, in this section, to propose the best prediction model, a Stacked ML-based prediction model using algorithms of ETR, BR, and LightGBM as an estimator is introduced, in which the best-predicted values for each floor level, are selected, and finally, the aggregate of the predictions is plotted. It should be noted that the proposed model has the ability to predict the ID of each floor level of BRBFs in parallel processing to reduce the time of calculations. Fig. 11 presents the predictions of the ID distribution of BRBFs using the proposed ML-based model assuming the median method (i.e., the middle value) for estimating the values of the distribution. It is observed that the proposed Stacked ML algorithm can accurately predict the ID distribution of all selected BRBFs with an accuracy of more than 98.3%, which is a good estimation tool for structural designers. Fig. 12 presents the predictions of the ID distribution of BRBFs using the proposed Stacked ML-based model assuming the mean method (i.e., the arithmetic average) for estimating the values of the distribution. Although there are differences between the median and mean methods of estimation of ID distribution, the proposed Stacked ML method can accurately predict the distribution in both methods which shows the capability of the proposed method. In addition, the predicted values of ID in each floor level can illustrate the weak story of the building, and the designer can use the results of the prediction to prevent this failure. Moreover, having the distribution of ID for a building (i.e., existing or newly constructed) can facilitate the retrofitting process and reduce the cost of retrofitting.

Although Figs. 11 and 12 can show the capability of the ML models, Tables 5 and 6 illustrate the error indicators for the ID distribution of the 6-Story BRBFs assuming the median and mean methods, respectively. To compare the ML models used in this research, Tables 5 and 6 can be used, in which it can be seen that the proposed Stacked ML has the highest R^2 value and the lowest error indicators compared to other ML models, which confirms the ability of model for estimating ID distribution. To better compare the time of execution of ML models, an algorithms has been added to the models to determine the execution time (i.e., see Tables 5 and 6). It can be seen that the Stacked ML model has the highest execution time compared to other models, since it has more base estimators and needs more time to aggregate the results. For brevity, other results of error indicators for the ID distribution of the 2-, to 12-Story BRBFs assuming the median and mean methods have been illustrated in Tables A-2 to A-11 in the *Appendix*, respectively.

Table 2
Hyperparameters of the Stacked ML algorithm.

Sub-Models	n_estimators	learning_rate	min_sample_leaf	min_sample_split	max_depth	random_state
XGBoost	3000	0.001	15	15	8	–
GBM	3500	0.01	10	8	5	–
LightGBM	800	0. 0001	–	–	5	–
ETR	800	–	5	10	–	0
BR	600	–	–	–	–	0
HGBR	2500	0.01	8	8	4	–
RF	2200	–	–	–	6	0

Table 3
Error indicators for evaluating the proposed Stacked ML algorithm (Kazemi et al., 2023c).

Indicator	Formula
Coefficient of determination	$R^2 = 1 - \frac{\sum_{i=1}^{n}(\text{Actual}_i - \text{Predicted}_i)^2}{\sum_{i=1}^{n}(\text{Actual}_i - \text{Actual}_{avg})^2}$
Mean squared error	$MSE = \frac{1}{n}\sum_{i=1}^{n}(\text{Actual}_i - \text{Predicted}_i)^2$
Mean absolute error	$MAE = \frac{1}{n}\sum_{i=1}^{n}\lvert\text{Actual}_i - \text{Predicted}_i\rvert$
Mean absolute relative error	$MARE = \frac{1}{n}\sum_{i=1}^{n}\left\lvert\frac{\text{Actual}_i - \text{Predicted}_i}{\text{Actual}_i}\right\rvert$
Mean square relative error	$MSRE = \frac{1}{n}\sum_{i=1}^{n}\left\lvert\frac{\text{Actual}_i - \text{Predicted}_i}{\text{Actual}_i}\right\rvert^2$
Root mean squared relative error	$RMSRE = \sqrt{\frac{1}{n}\sum_{i=1}^{n}\left(\frac{\text{Actual}_i - \text{Predicted}_i}{\text{Actual}_i}\right)^2}$
Mean bias error	$MBE = \frac{1}{n}\sum_{i=1}^{n}(\text{Actual}_i - \text{Predicted}_i)$
Maximum absolute relative error	$\text{erMAX} = \max\left(\left\lvert\frac{\text{Actual}_i - \text{Predicted}_i}{\text{Actual}_i}\right\rvert\right)$
Standard deviation	$SD = \sqrt{\frac{\sum(X_i - \text{Arithmetic mean})^2}{\text{total number}}}$

4.4. Comparing prediction methods

There are two famous prediction formulas, namely as FEMA P-58 method (FEMA P-58, 2012) and Erochko et al. (2011), which are widely used by researchers to estimate the RID of BRBFs. Following FEMA P-58 method (FEMA P-58, 2012), the median of RID, Δ_r, is estimated as follows for each story of the building:

$$\Delta_r = 0 \;\; \Delta \le \Delta_y \tag{2}$$

$$\Delta_r = 0.3(\Delta - \Delta_y) \;\; \Delta_y < \Delta < 4\Delta_y$$

$$\Delta_r = (\Delta - 3\Delta_y) \;\; \Delta \ge 4\Delta_y$$

where, for each story of the BRBF, Δ and Δ_y illustrate the maximum ID and story yield drift ratio, respectively. According to FEMA P-58 (FEMA P-58, 2012), the Δ value for each floor of a structure, determined from NTHA, can be used to estimate Δ_r using Equation (2). Section 5.3 of FEMA P-58 (FEMA P-58, 2012) provides a simplified method of determining Δ using linear static analysis. In addition, nonlinear static pushover analysis can be used for determining the Δ_y.

According to the proposed equation by Erochko et al. (2011), the mean of RID for steel MRFs and BRBFs, $\Delta_{r,\,mean}$, for each floor of the structure is determined as follows:

$$\Delta_{r,mean} = (\Delta_{\max} - \Delta_y) \times \frac{DCF}{2.5} \;\; \Delta_{r,mean} < \Delta_{r,\max} \tag{3}$$

where $\Delta_{\max}$ and Δ_y are the mean of ID for each story of the buildings by performing NTHA and the story yield drift ratio, respectively. The drift concentration factor, which is the ratio of maximum ID to maximum roof drift, should be less than 2.5 in Equation (3).

As in the real condition, it is not possible to have access to the actual values of maximum RID, hence, the predictions made by seismic provisions are considered as a main source for designing purposes. Although some studies have introduced a formula for estimating the maximum RID of BRBFs, there are still differences between the actual and estimated values of the RID of BRBFs (e.g., see (Asgarkhani et al., 2020)). In other words, the proposed formulas have a conservative estimation of maximum RID that may affect the designing procedures. In this study, a comparison has been conducted between the actual values of the maximum RID and the estimated values by formulas and an ML-based prediction model.

In Fig. 13, the median of RID obtained from the NTHA (i.e., actual values) and those predicted by the FEMA P-58 (FEMA P-58, 2012) method and ML-based method are compared for the BRBFs having different values of α, R and the bay length. It is noteworthy that the maximum value of the distribution of RID in BRBFs plays a key role in the designing of assumptions and structural elements. ML-based methods predicted the maximum of the median of RID with higher accuracy than FEMA P-58 (FEMA P-58, 2012). It can be seen that similar trends are observed in the results of other BRBFs. For instance, the predicted value of the maximum of the median IRD by FEMA P-58 (FEMA P-58, 2012) method for 2-Story BRBF is 0.365%, whereas ML-based models estimated 0.206% for this story, which is 2.12 and 1.2 times larger than the actual value, respectively. In 4-Story BRBF, the maximum of the median of RID predicted by FEMA P-58 (FEMA P-58, 2012) is equal to 0.163%, which belongs to the four-floor level, while the predicted value by the ML model is 0.112%, which is fitted to the actual value. According to the results, the calculated values by FEMA P-58 (FEMA P-58, 2012) for the 8-Story BRBF in the sixth floor is equal to 0.376%, which is 2.46 times higher than the corresponding actual value of 0.153%. Based on the ML method, the predicted value for the sixth floor is 0.166% which is 1.08 times larger than the corresponding actual value.

Table 4
Results of error indicators for the pre-processing dataset assuming ML models.

ML algorithm	R^2	MSE	MAE	MARE	MSRE	RMSRE	MBE	erMAX	SD
XGBoost	0.904	2.68	1.67	0.21	0.036	0.21	0.32	0.72	0.01
RF	0.913	2.36	1.56	0.19	0.053	0.18	0.41	0.46	0.01
BR	0.941	2.18	1.13	0.15	0.014	0.12	0.26	0.23	0.01
ETR	0.964	2.11	1.15	0.11	0.027	0.07	0.16	0.11	0.01
GBM	0.871	3.15	1.89	0.31	0.282	0.78	0.46	1.37	0.01
ANNs	0.943	2.18	1.17	0.15	0.034	0.14	0.27	0.28	0.01
RNNs	0.932	2.24	1.26	0.16	0.041	0.15	0.33	0.37	0.01
Stacked ML	0.988	2.01	1.04	0.09	0.023	0.05	0.11	0.07	0.01

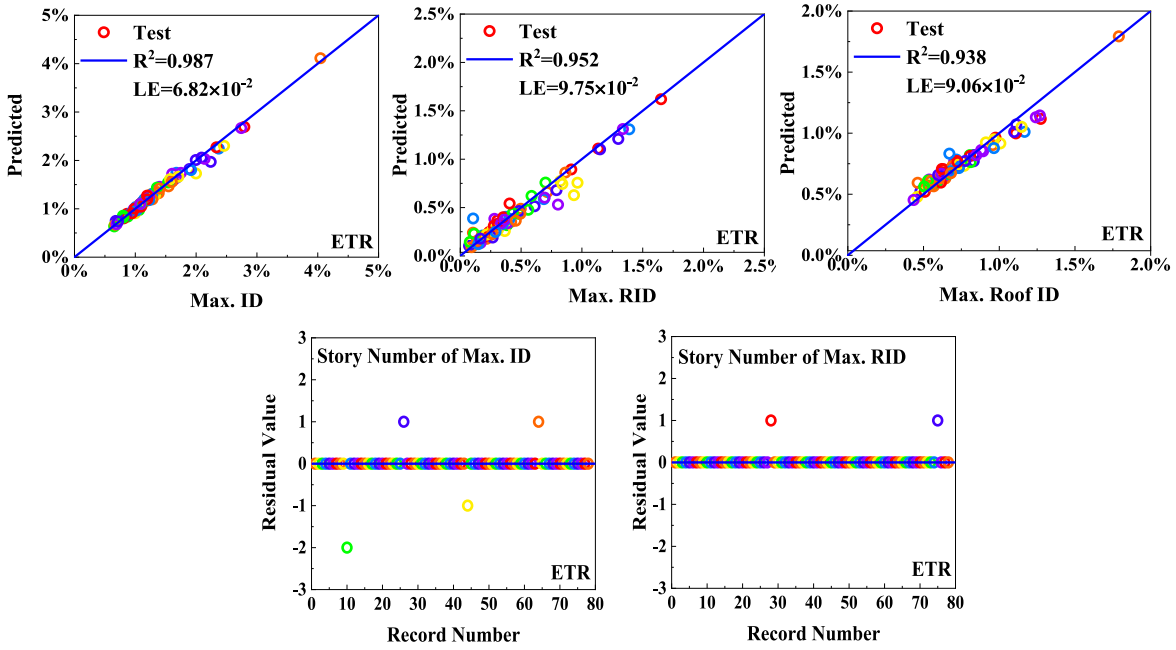

Fig. 9. Response predictions of the 4-Story BRBF with $\alpha = 0.003$, $R = 4$, and bay length of 9.14 m using the ETR algorithm.

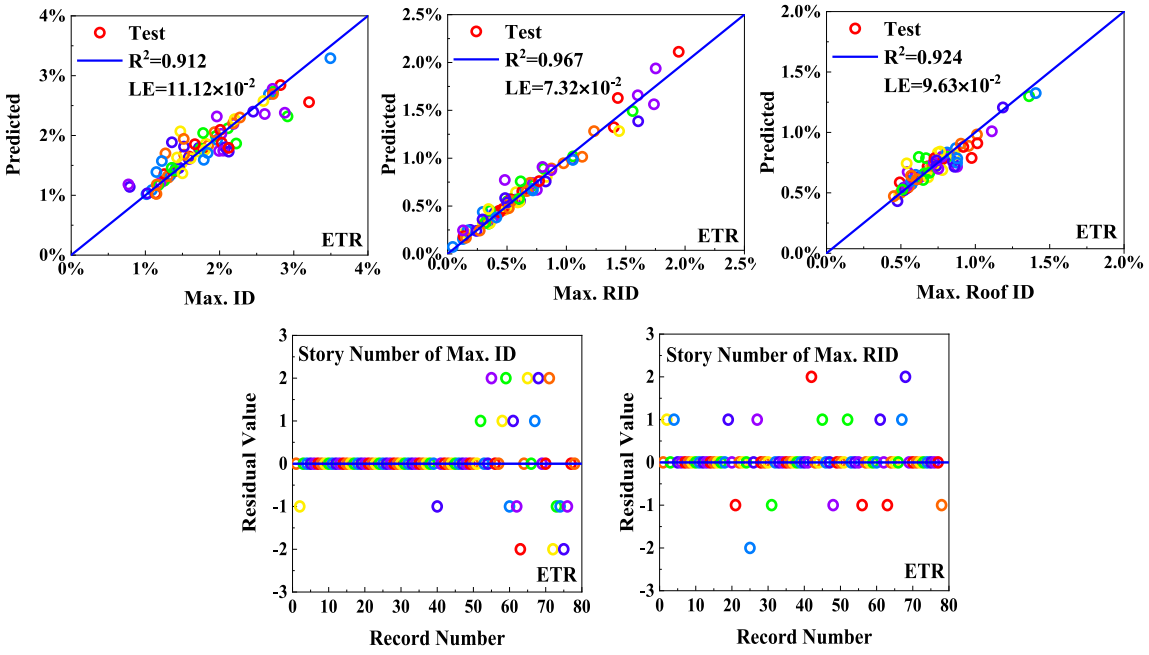

Fig. 10. Response predictions of the 8-Story BRBF with $\alpha = 0.01$, $R = 3$, and bay length of 7.32 m using the ETR algorithm.

Fig. 14 illustrates the predictions of the RID distribution of BRBFs using the proposed Stacked ML-based model assuming the mean method. Similar to the median method, it can be observed that the Erochko et al. (2011) method has a conservative estimation of RID distribution, while the ML-based prediction model can estimate the RID of floor levels fitted to the actual values. For example, for the six-floor level of the 6-Story BRBF, the RID of 0.94% determined by Erochko et al. (2011) is 4.24 and 3.54 times of actual and ML predicted values, respectively, while the ML predicted value is 1.19 times of the actual value. Considering the obtained results, FEMA P-58 (FEMA P-58, 2012) and Erochko et al. (2011) provide conservative estimations for the distribution of RID in most cases. Nevertheless, the RID values predicted by the proposed Stacked ML-based model are significantly closer to those actual values and can be selected as the best prediction model among other ML models.

Tables 7 and 8 illustrate the error indicators for the RID distribution of the 6-Story BRBFs assuming the median and mean methods, respectively. It can be observed that the proposed Stacked ML have the highest R^2 value and the lowest error indicators compared to other ML models. Moreover, the proposed Stacked ML can perform better than individual ML models and can be used to compensate for the ability of equations used for estimating RID distribution. However, the execution time of the

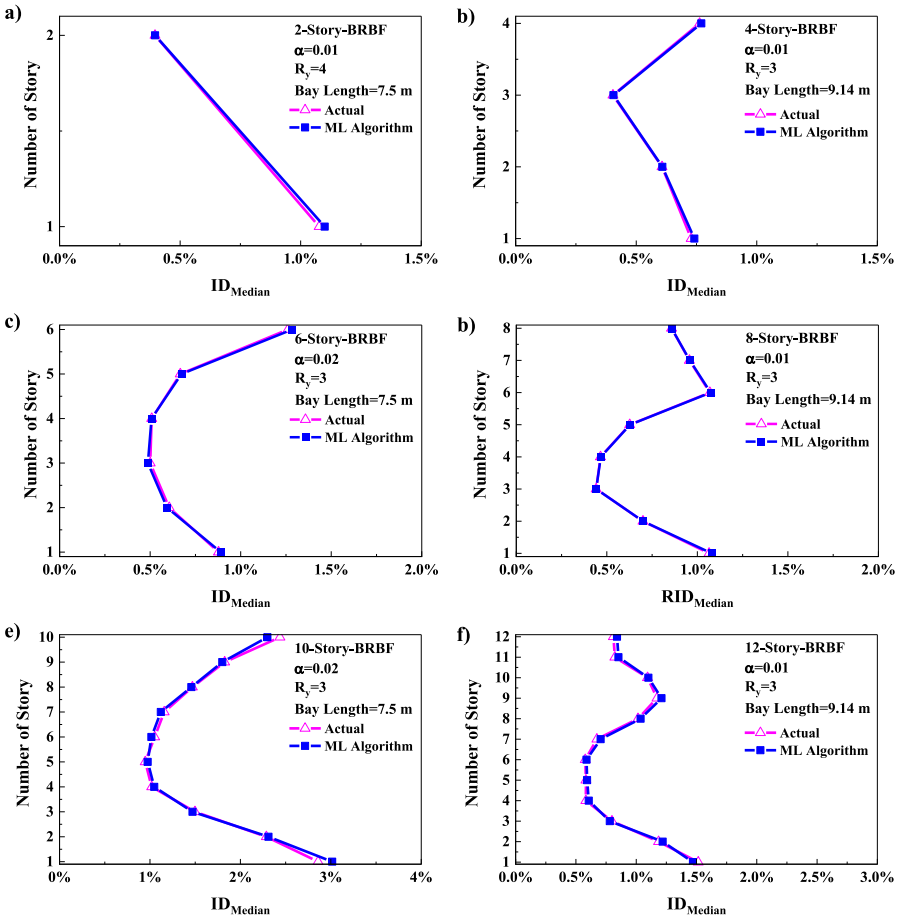

Fig. 11. Predictions of the ID distribution of BRBFs using the proposed Stacked ML-based model assuming the median method.

Stacked ML model is higher than other models. For brevity, other results of error indicators for the RID distribution of the 2-, to 12-Story BRBFs assuming the median and mean methods have been illustrated in Tables A-12 to A-21 in *Appendix*, respectively.

4.5. Seismic performance prediction

It has been illustrated in the previous subsections that the proposed ML method, as one of the twenty ML algorithms used by authors (for more detail see (Kazemi et al., 2023a; Kazemi et al., 2023b; Kazemi et al., 2023c)) has been enhanced to accurately predict the distribution of ID and RID assuming two methods of mean and median, which considerably improved the formula that is available for the same purpose (i.e., FEMA P-58 and Erochko methods). Then, the ML method's ability is improved for predicting the median of IDA curves of BRBFs. Fig. 15 presents the comparison of the ML-based prediction models for estimating the median of IDA curves of the 4-, and 6-Story BRBFs. It can be observed that in both BRBFs, the ANNs have an accurate estimation of the median of IDA curves and can be used for prediction purposes. Although the results of the 4-, and 6-Story BRBFs are discussed in this section, similar results were observed for other BRBFs. Therefore, two methods of ANNs and ETR are introduced as the best prediction models, which can estimate the performance of BRBFs. For instance, in the maximum ID of 10%, the ANNs can estimate the collapse performance of the 4-, and 6-Story BRBFs with an accuracy of 97.69% and 98.96%, respectively.

4.6. Prediction of seismic failure probability

Although predicting the performance curve of BRBFs can improve the knowledge of buildings, it cannot be used for seismic risk assessment or plotting the seismic fragility curve. Therefore, in this section, the ability of the ML algorithms has been improved for failure probability assessment. Fig. 16 illustrates the comparison of the proposed prediction model for estimating the failure probability of collapse performance of the 4-, and the 6-Story BRBFs using ML algorithms. According to Fig. 16 (a), the ETR and XGBoost algorithms have been fitted to the actual curve of the seismic collapse probability (i.e., ID = 10%). For example, in the 50% failure probability (i.e., 0.5), the ETR, XGBoost and ANNs algorithms achieved values of 2.9, 2.87, and 3.05, respectively, which have 1.36%, 2.38%, and 3.74% differences compared to the actual value of 2.94, respectively. According to Fig. 16(b), in the 50% failure probability (i.e., 0.5), the XGBoost, ETR, and ANNs algorithms achieved values of 1.41, 1.4, and 1.46, respectively, which have 1.39%, 2.09%, and 2.09% differences compared to the actual value of 1.43, respectively, and can be selected as the best prediction models. Therefore, the results showed that the seismic failure probability of BRBFs can be determined based on the ML algorithms and can be used for estimating the seismic risk and vulnerability of buildings. The proposed algorithms can accelerate the seismic risk and vulnerability assessment of buildings for designing and retrofitting purposes.

5. General use of the proposed ML-based model

The previously prescribed formulas by FEMA P-58 (FEMA P-58, 2012) and Erochko et al. (2011) can provide information on ID and RID

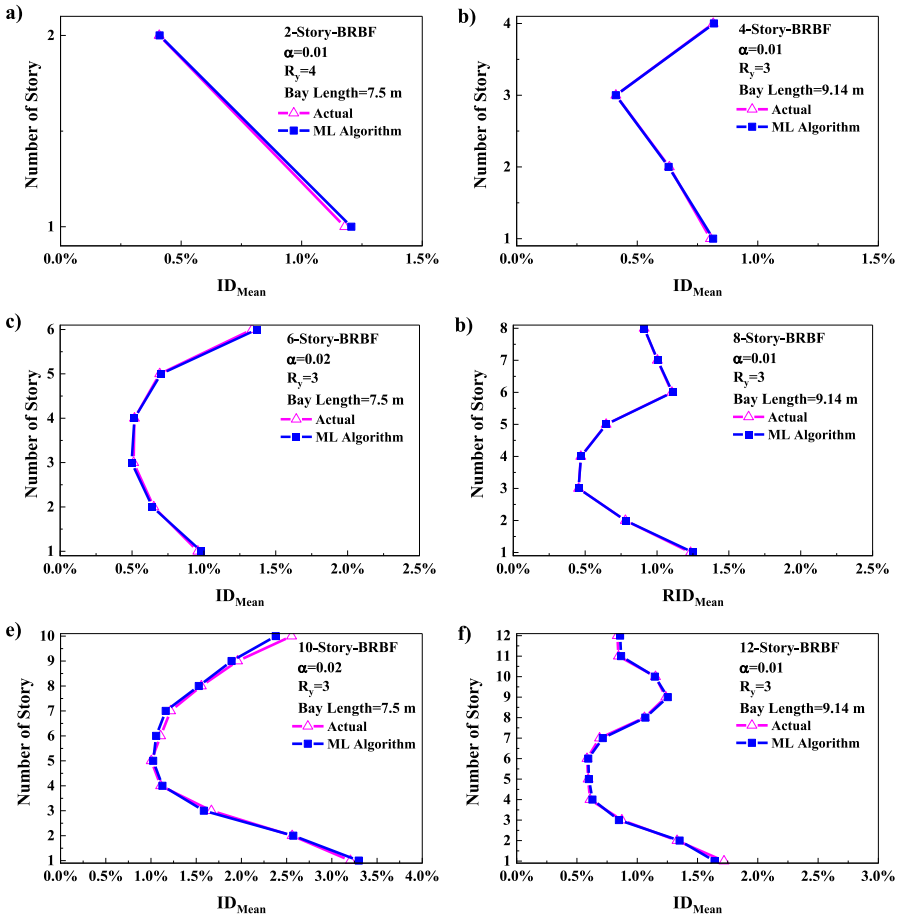

Fig. 12. Predictions of the ID distribution of BRBFs using the proposed Stacked ML-based model assuming the mean method.

Table 5
Results of error indicators for the ID distribution of the 6-Story BRBFs assuming the median method.

ML algorithm	R^2	MSE	MAE	MARE	MSRE	RMSRE	MBE	erMAX	SD	Execution time (sec)
XGBoost	0.912	2.57	1.77	0.205	0.534	0.053	0.06	0.052	0.022	467
RF	0.915	2.43	1.76	0.201	0.523	0.053	0.06	0.052	0.022	356
BR	0.952	2.24	1.37	0.180	0.367	0.033	0.05	0.039	0.015	432
ETR	0.972	2.03	1.22	0.160	0.303	0.021	0.04	0.029	0.015	312
GBM	0.901	3.19	1.94	0.213	0.580	0.071	0.08	0.078	0.019	544
ANNs	0.921	2.59	1.72	0.192	0.403	0.046	0.06	0.047	0.017	612
RNNs	0.954	2.19	1.35	0.186	0.368	0.028	0.05	0.038	0.016	667
Stacked ML	0.983	1.85	1.17	0.154	0.294	0.017	0.03	0.026	0.015	753

Table 6
Results of error indicators for the ID distribution of the 6-Story BRBFs assuming the mean method.

ML algorithm	R^2	MSE	MAE	MARE	MSRE	RMSRE	MBE	erMAX	SD	Execution time (sec)
XGBoost	0.915	4.51	1.69	0.63	0.521	0.03	0.093	0.036	0.031	495
RF	0.912	4.56	1.83	0.65	0.527	0.03	0.093	0.036	0.031	370
BR	0.955	3.84	1.88	0.31	0.488	0.02	0.081	0.032	0.024	445
ETR	0.962	3.68	1.73	0.23	0.465	0.02	0.077	0.029	0.021	312
GBM	0.883	5.78	1.92	0.83	0.751	0.05	0.124	0.047	0.053	525
ANNs	0.947	3.96	1.17	0.42	0.498	0.02	0.087	0.032	0.024	598
RNNs	0.951	3.84	1.19	0.32	0.492	0.02	0.082	0.032	0.024	689
Stacked ML	0.991	3.52	1.53	0.180	0.405	0.020	0.073	0.027	0.019	780

distribution along the floor levels, while these formulas have limitations. For instance, there is still a need to model the BRBF and this may take time to provide the results for new input parameters. In addition, by changing the input parameters, the total process should be conducted again; thus, the predictions made by these formulas cannot be used for fast assessment of buildings. To overcome the shortcomings of existing formulas, ML-based prediction models have been introduced that can be used for estimating different seismic responses of BRBFs without limitation on the number of uses and for different ranges of input parameters. Moreover, to include all results of this study, a preliminary

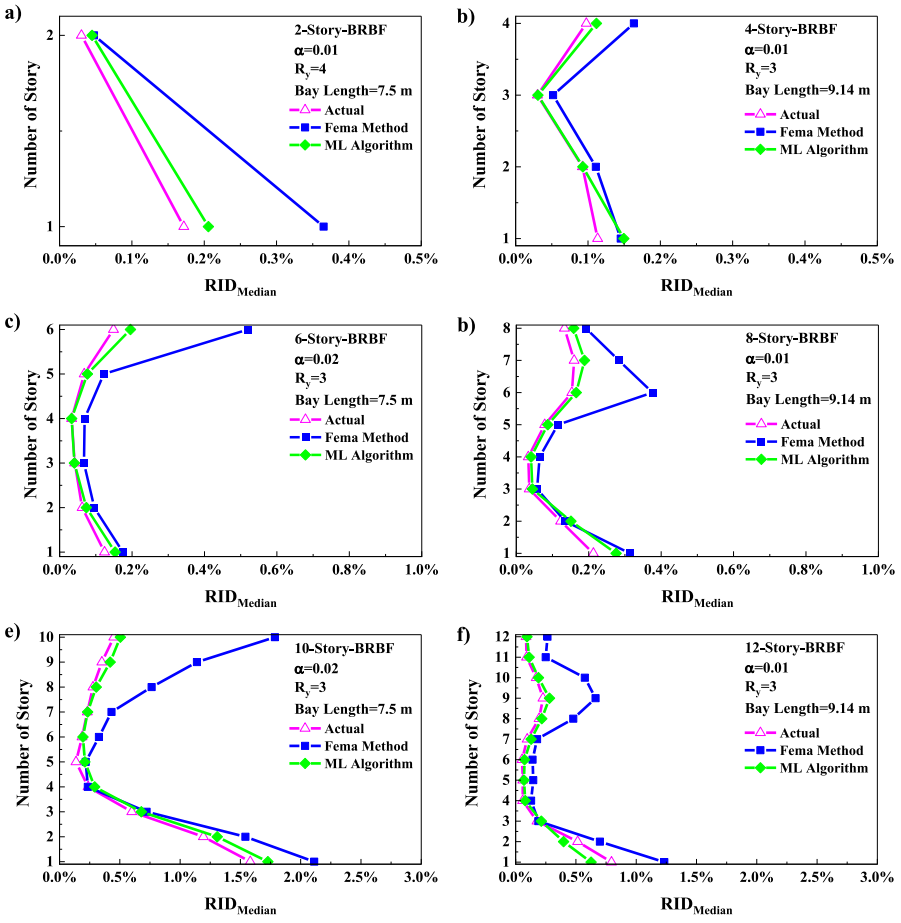

Fig. 13. Predictions of the RID distribution of BRBFs using the proposed Stacked ML-based model assuming the median method.

prediction tool for using the proposed ML algorithms to predict the seismic response and performance curves of BRBFs is presented in Fig. 17. Using this tool can facilitate the seismic behavior assessment of BRBFs in the purpose of designing or retrofitting buildings. Moreover, the possibility of plotting the distribution curves of the ID and RID can provide information for structural designers. It is possible to predict the failure probability curve and use the curve to assess the seismic risk and vulnerability of BRBFs. Estimating proposed in the paper can facilitate the process of design and analysis while improving the knowledge of engineers about the current state of the building. The current study investigates the BRBFs having two-, to twelve-story elevations with different bay lengths. Although the authors tried to prepare a wide range of dataset with reasonable lengths and story elevations, the proposed GUI has some limitations in use for the BRBFs with higher than twelve-story elevation, and having bigger span length than 9.14 m or lower span length than 7.32 m. It should be noted that this tool could estimate the outputs for the input parameters of the BRBFs that have the values between the predefined two groups. Moreover, due to the capability of the proposed GUI to use the database, it is possible to update the database in future studies to improve the limitations.

The GUI developed in this study serves as a powerful tool to assess and enhance the seismic performance of buildings, specifically focusing on BRBFs. The GUI is designed to address the shortcomings of existing seismic response estimation formulas and provide a comprehensive approach to predict seismic responses effectively. For instance, when facing the challenge of unpredictable values of RID during seismic events, civil engineers can utilize the GUI to optimize the performance of a building. The interface allows for retrofitting schemes such as strengthening beam-to-column connections, incorporating outer frame infills to resist lateral deformations, and integrating viscous dampers as dissipative devices and show how they can affect the building. These interventions are essential to ensure the building's resilience and safety in the face of seismic stress.

Moreover, the GUI tackles the limitations of existing formulas, such as time-consuming calculations and inflexibility in handling varying input parameters. Engineers can input specific parameters related to BRBFs into the interface, allowing them to quickly estimate seismic responses without the constraints of traditional formulas. The use of ML-based prediction models within the GUI further enhances accuracy and efficiency, enabling rapid assessment and aiding in the design or retrofitting of buildings. One notable feature of the GUI is its ability to provide graphical representations of the seismic response and performance curves of BRBFs. Engineers can easily interpret these curves, aiding in risk assessment and vulnerability analysis. Additionally, the tool predicts failure probability curves, providing crucial insights to assess seismic risk comprehensively.

However, it is important to note that the GUI does have certain limitations, specifically concerning building specifications. For buildings with more than twelve-story elevations or span lengths beyond the defined range, the tool may not provide accurate estimations. Despite these limitations, the GUI's flexibility in utilizing a database allows for potential updates and improvements in future studies, demonstrating its adaptability and potential for ongoing refinement to better serve engineering needs.

6. Conclusions

This research has been focused on ML-based prediction models since

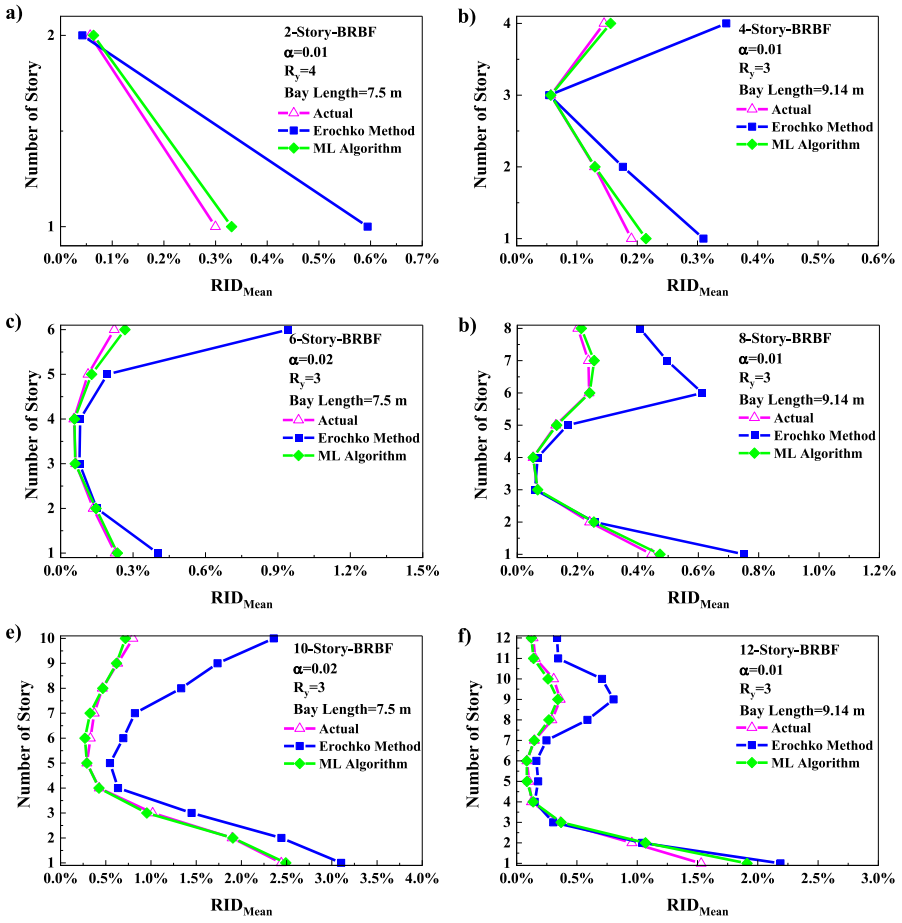

Fig. 14. Predictions of the RID distribution of BRBFs using the proposed Stacked ML-based model assuming the mean method.

Table 7
Results of error indicators for the RID distribution of the 6-Story BRBFs assuming the median method.

ML algorithm	R^2	MSE	MAE	MARE	MSRE	RMSRE	MBE	erMAX	SD	Execution time (sec)
XGBoost	0.934	2.66	1.29	0.47	0.598	0.04	0.13	0.05	0.03	506
RF	0.907	3.55	1.54	0.72	0.637	0.07	0.18	0.07	0.03	381
BR	0.956	2.33	1.13	0.38	0.591	0.04	0.09	0.04	0.02	459
ETR	0.964	2.02	1.15	0.31	0.583	0.03	0.09	0.04	0.02	301
GBM	0.929	3.21	1.41	0.51	0.618	0.05	0.15	0.05	0.03	511
ANNs	0.933	2.68	1.3	0.47	0.601	0.04	0.13	0.05	0.03	613
RNNs	0.941	2.24	1.23	0.42	0.598	0.04	0.10	0.05	0.02	701
Stacked ML	0.975	1.43	1.12	0.24	0.572	0.03	0.09	0.04	0.02	799

Table 8
Results of error indicators for the RID distribution of the 6-Story BRBFs assuming the mean method.

ML algorithm	R^2	MSE	MAE	MARE	MSRE	RMSRE	MBE	erMAX	SD	Execution time (sec)
XGBoost	0.938	1.57	1.07	0.55	0.663	0.06	0.07	0.21	0.01	572
RF	0.921	1.66	1.01	0.51	0.665	0.06	0.07	0.26	0.01	435
BR	0.965	1.32	0.80	0.43	0.528	0.05	0.06	0.18	0.01	508
ETR	0.971	1.29	0.81	0.35	0.533	0.05	0.06	0.12	0.01	366
GBM	0.932	1.59	1.18	0.75	0.618	0.06	0.07	0.21	0.01	601
ANNs	0.918	1.77	0.82	0.63	0.738	0.07	0.07	0.31	0.01	712
RNNs	0.925	1.65	0.86	0.45	0.660	0.06	0.07	0.21	0.01	823
Stacked ML	0.983	1.13	0.61	0.39	0.417	0.05	0.06	0.09	0.01	878

there is a need for fast estimation of the seismic behavior and seismic performance of BRBFs in retrofitting procedures. For this purpose, two main groups of BRBFs, having different types of parameters, were designed and modeled in OpenSees (McKenna et al., 2015) software. Then, 78 far-field ground motions suitable for the constructional site were used to perform NTHAs and IDAs based on the ID and RID demands. Different types of demands were determined and defined as a training dataset for the ML methods. Twenty ML algorithms were used to

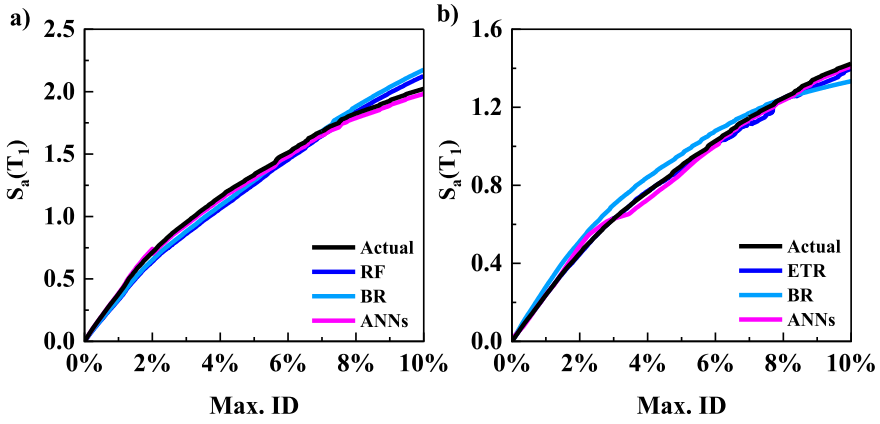

Fig. 15. Comparing the ability of the proposed prediction models for estimating the median of IDA curves of, a) the 4-Story, and b) the 6-Story BRBFs using ML algorithms.

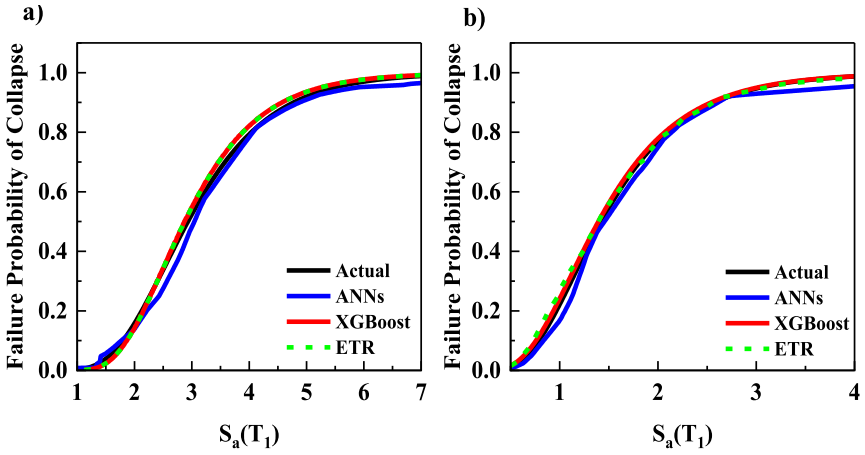

Fig. 16. Comparing the ability of the proposed prediction model for estimating the failure probability of collapse performance of, a) the 4-Story, and b) the 6-Story BRBFs using ML algorithms.

find out the best of them for the prepared training datasets. The ML models with the best results of error indicators were investigated, as well as, a combination of ML algorithms as a Stacked ML model was introduced for predicting the distribution of seismic responses. The PDP of input features shows that increasing the weight, number of stories, and building height have small effects on the prediction of seismic responses, while the increase in base shear, T_1 and R_y lead to an increase in the prediction of seismic responses, although the effects of R_y is more evident as compared to others. Moreover, by increasing the values of γ and α, their effects are reduced correspondingly. The proposed ML-based prediction model has the ability to predict seismic responses with the highest accuracy. For example, the ETR algorithm can predict the maximum ID, maximum RID and maximum roof ID with the accuracy of 98.7%, 95.2%, and 93.8%, respectively, for the 4-Story BRBF with $\alpha = 0.003$, $R = 4$, and bay length of 9.14 m. To improve the ability of the ML algorithms, a combination of estimators, such as the ANNs, RNNs, ETR, BR, HGBR, GBM, XGBoost, and LightGBM that have higher accuracy, were used to provide a Stacked ML-based prediction model. The proposed prediction model can improve the capability of existing ML algorithms in terms of predicting the distribution of ID and RID along the floor levels of BRBFs while using parallel processing to reduce the time of calculations. For example, the proposed Stacked ML can estimate the ID distribution of BRBFs with an accuracy of more than 98.3% in both the median and mean methods. Nevertheless, the RID values predicted by the proposed ML-based model have been fitted to the actual values. Since the seismic performance curve of BRBFs can provide information regarding the performance levels of the building, the ML models have been improved to predict the median of IDA curves. The results show that the ANNs can estimate the total collapse performance level of the 4-, and the 6-Story BRBFs (i.e., in the maximum ID of 10%) with the accuracy of 97.69% and 98.96%, respectively. The seismic failure probability curve can be used for seismic risk and vulnerability assessment of buildings. In this research, the plot curve ability of the prediction models has been improved to provide the seismic fragility curve of BRBFs. For example, in the 50% failure probability (i.e., 0.5) of the 4-Story BRBF, the ETR, XGBoost and ANNs algorithms have achieved values of 2.9, 2.87, and 3.05, respectively, which are different by 98.63%, 97.61%, and 96.25%, as compared to the actual value of 2.94. The preliminary estimation tool has been introduced to provide predictions based on the input parameters introduced in this study. In addition, it should be noted that this tool has the ability to estimate the outputs for the input parameters of the BRBFs that have the values between the predefined two groups.

For future studies, the authors suggested to use near-field ground motions suitable for the constructional site considering pulse-like and no-pulse effects. In addition, it would be better if more attempts had been carried out to take the hazard curves into account and improve the capability of the GUI for estimating the mean annual rate of exceedance of an intensity measure. Although the authors tried to provide a wide range of dataset, there is still a room to model more structures to provide

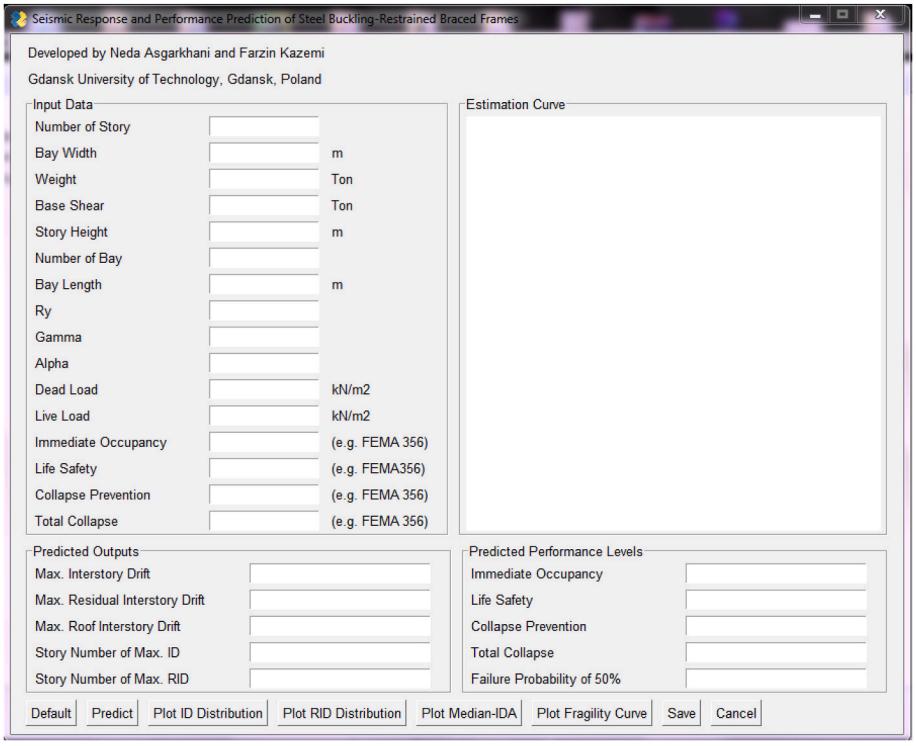

Fig. 17. The preliminary prediction tool for using the proposed ML algorithms to predict the seismic response and performance curves of BRBFs (available at https://github.com/FarzinKazemi).

a complete range of input features.

CRediT authorship contribution statement

N. Asgarkhani: Investigation, Data curation, Resources, Methodology, Formal analysis, Software, Validation, Conceptualization, Visualization, Writing – original draft. **F. Kazemi:** Conceptualization, Methodology, Formal analysis, Software, Resources, Data curation, Investigation, Project administration, Validation, Visualization, Writing – original draft. **A. Jakubczyk-Gałczyńska:** Supervision, Writing – review & editing. **B. Mohebi:** Supervision, Software, Writing – review & editing. **R. Jankowski:** Supervision, Writing – review & editing.

Declaration of competing interest

The authors did not receive support from any organization for the submitted work. The authors have no relevant financial or non-financial interests to disclose.

The authors declare that there is no conflict of interest with relation to the paper **'Seismic response and performance prediction of steel buckling-restrained braced frames using machine-learning methods'** submitted for publication in *Engineering Applications of Artificial Intelligence*. All authors agreed with the content and that all gave explicit consent to submit the paper.

Data availability

Data will be made available on request.

Acknowledgement

The authors would like to express very great appreciation and to acknowledge Dr. Mansoor Yakhchalian for his efforts and helps during the modelling process. Numerical calculations were carried out at the Tri-City Academic Supercomputer and Network (*CI TASK*) in Gdańsk, Poland.

Appendix

Table A-1 presents the abbreviations and acronyms list used in this research.

Table A-1
Abbreviations and acronyms list used in the research.

Abbreviation	Description
BRB	Buckling restrained brace
ID	Interstory drift
RID	Residual interstory drift
BRBFs	Buckling-restrained brace frames
MRF	Moment Resisting Frames
NTHA	Nonlinear time-history analysis
IDA	Incremental dynamic analysis

(*continued on next page*)

Table A-1 (*continued*)

Abbreviation	Description
DBE	Design-based earthquake level
MCE	Maximum considered earthquake level
ML	Machine learning
ANNs	Artificial Neural Networks
RNNs	Recurrent Neural Networks
RF	Random Forest
ETR	Extra-Trees Regressor
BR	Bagging Regressor
GBM	Gradient Boosting Machine
AdaBoost	Adaptive Boosting
XGBoost	Extreme Gradient Boosting
HGBR	Histogram-based Gradient Boosting Regression
PDP	Partial Dependence Plot
TPOT	Tree-based Pipeline Optimization Tool
ID_{Med}	Median of interstory drift
RID_{Med}	Median of residual drift
$Sa(T_1)$	Spectral acceleration at fundamental period of structures
SD_S and SD_1	Spectral acceleration for the considered design site

Figs. A-1 and A-2 present the details of BRBFs with bay lengths of 7.32 m and 9.14 m in the X-direction, respectively.

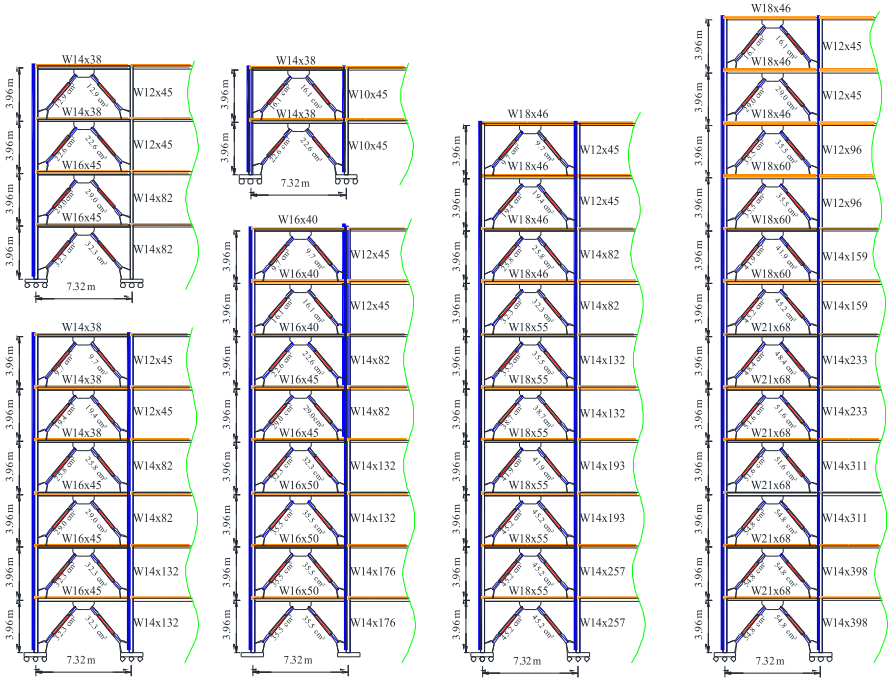

Fig. A-1. Details of BRBFs with the bay length of 7.32 m in the X-direction.

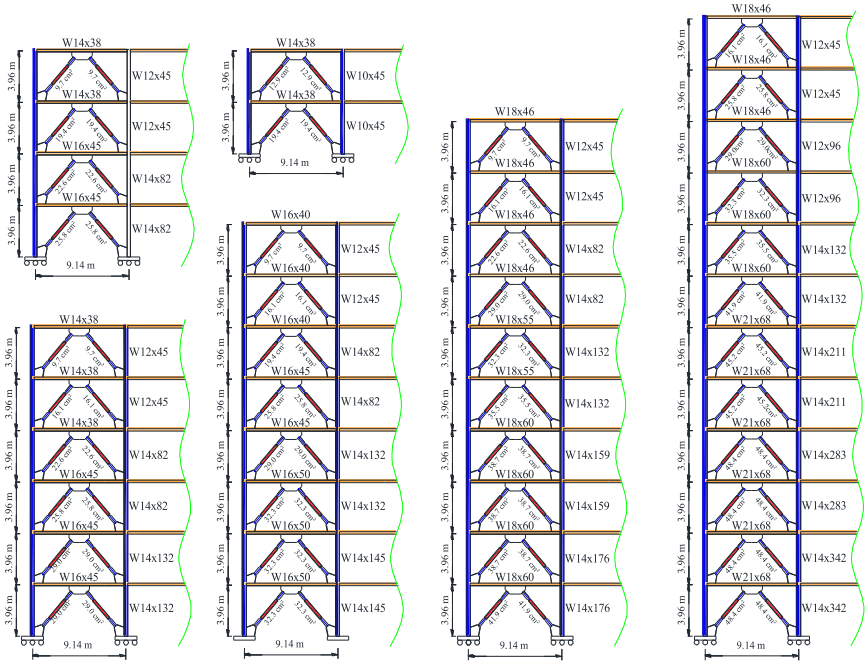

Fig. A-2. Details of BRBFs with the bay length of 9.14 m in the X-direction.

Pseudo-code provides a simplified representation of the process of ML model; therefore, following procedure can be used to represent the Stacked ML model used in this research.

Algorithm: Stacked ML with TPOT and Feature Selection

Input:

- Dataset with input features X and target variable Y
- Hyperparameters optimization algorithm: TPOT
- Feature selection methods: filter, wrapper, embedded
- ML models for base and meta-level: Base_Models, Meta_Model

Output:

- Stacked ensemble model

Initialize:

- Selected_Features = Feature_Selection(X, Y) #Select relevant features based on the preprocessing
- Optimized_Hyperparameters = TPOT_Optimize(X[Selected_Features], Y) #Optimize hyperparameters
- Base_Models = Train_Base_Models (X[Selected_Features], Y, Optimized_ Hyperparameters) # Train base models

Train Stacked ML Model:

- Split the dataset into training and validation sets: X_train, X_val, Y_train, Y_val
- Initialize an empty array to store meta-level training data: X_meta_train = []
  For i = 1 to len(Base_Models):
  - Fit Base_Models[i] on X_train and predict on X_val: base_model_predictions
  - Append base_model_predictions to X_meta_train
- Train the Meta_Model on X_meta_train and Y_val
- Return the ensemble model with Base_Models and Meta_Model

Prediction (for a new instance X_new):

- Base_Model_Predictions = []
- For each base model in Base_Models:
- Predict using the base model for X_new and append to Base_Model_Predictions

- Predict using Meta_Model for Base_Model_Predictions
- Return the final prediction

Results of error indicators for the ID and RID distribution of the 2-, to 12-Story BRBFs assuming the median and mean methods have been presented in Tables A-2 to A-21, respectively.

Table A-2
Results of error indicators for the ID distribution of the 2-Story BRBFs assuming the median method.

ML algorithm	R^2	MSE	MAE	MARE	MSRE	RMSRE	MBE	erMAX	SD	Execution time (sec)
XGBoost	0.945	2.23	1.58	0.195	0.515	0.05	0.06	0.048	0.021	526
RF	0.938	2.34	1.53	0.191	0.507	0.05	0.06	0.047	0.021	415
BR	0.958	2.04	1.29	0.16	0.398	0.04	0.05	0.036	0.016	492
ETR	0.985	1.81	1.15	0.132	0.302	0.02	0.04	0.027	0.014	334
GBM	0.922	2.76	1.74	0.204	0.543	0.07	0.08	0.06	0.018	586
ANNs	0.953	2.23	1.48	0.182	0.419	0.04	0.06	0.044	0.017	611
RNNs	0.962	1.92	1.25	0.146	0.314	0.03	0.05	0.032	0.015	672
Stacked ML	0.991	1.45	1.06	0.121	0.261	0.01	0.03	0.02	0.013	753

Table A-3
Results of error indicators for the ID distribution of the 2-Story BRBFs assuming the mean method.

ML algorithm	R^2	MSE	MAE	MARE	MSRE	RMSRE	MBE	erMAX	SD	Execution time (sec)
XGBoost	0.959	2.18	1.56	0.193	0.513	0.05	0.06	0.047	0.021	478
RF	0.945	2.29	1.52	0.187	0.503	0.05	0.06	0.046	0.021	389
BR	0.958	1.96	1.25	0.154	0.392	0.03	0.05	0.035	0.016	455
ETR	0.954	1.79	1.26	0.124	0.285	0.02	0.04	0.026	0.014	307
GBM	0.928	2.66	1.64	0.234	0.531	0.06	0.08	0.058	0.018	548
ANNs	0.966	2.11	1.42	0.176	0.407	0.04	0.06	0.042	0.017	602
RNNs	0.973	1.76	1.21	0.139	0.301	0.03	0.05	0.031	0.015	691
Stacked ML	0.997	1.29	1.03	0.109	0.245	0.01	0.03	0.018	0.012	731

Table A-4
Results of error indicators for the ID distribution of the 4-Story BRBFs assuming the median method.

ML algorithm	R^2	MSE	MAE	MARE	MSRE	RMSRE	MBE	erMAX	SD	Execution time (sec)
XGBoost	0.932	2.03	1.52	0.191	0.510	0.05	0.06	0.047	0.021	486
RF	0.916	2.15	1.47	0.184	0.500	0.05	0.06	0.046	0.021	370
BR	0.947	1.85	1.21	0.149	0.382	0.03	0.05	0.034	0.016	441
ETR	0.958	1.62	1.06	0.120	0.276	0.02	0.04	0.025	0.014	321
GBM	0.902	2.52	1.59	0.196	0.523	0.06	0.08	0.057	0.018	556
ANNs	0.935	1.99	1.37	0.172	0.396	0.04	0.06	0.041	0.017	578
RNNs	0.950	1.71	1.15	0.132	0.288	0.03	0.05	0.032	0.015	678
Stacked ML	0.965	1.24	1.02	0.107	0.239	0.01	0.03	0.018	0.012	715

Table A-5
Results of error indicators for the ID distribution of the 4-Story BRBFs assuming the mean method.

ML algorithm	R^2	MSE	MAE	MARE	MSRE	RMSRE	MBE	erMAX	SD	Execution time (sec)
XGBoost	0.943	1.86	1.45	0.187	0.502	0.05	0.06	0.047	0.021	502
RF	0.927	2.02	1.42	0.182	0.495	0.05	0.06	0.046	0.021	375
BR	0.954	1.76	1.18	0.145	0.375	0.03	0.05	0.033	0.016	421
ETR	0.959	1.57	1.05	0.116	0.270	0.02	0.04	0.024	0.014	309
GBM	0.912	2.42	1.55	0.192	0.516	0.06	0.08	0.057	0.018	568
ANNs	0.942	1.92	1.33	0.164	0.386	0.04	0.06	0.04	0.017	632
RNNs	0.953	1.67	1.12	0.128	0.280	0.03	0.05	0.029	0.015	691
Stacked ML	0.958	1.21	1.01	0.105	0.234	0.01	0.03	0.017	0.012	734

Table A-6
Results of error indicators for the ID distribution of the 8-Story BRBFs assuming the median method.

ML algorithm	R^2	MSE	MAE	MARE	MSRE	RMSRE	MBE	erMAX	SD	Execution time (sec)
XGBoost	0.939	2.16	1.39	0.175	0.491	0.05	0.06	0.046	0.021	483
RF	0.920	2.31	1.34	0.17	0.484	0.05	0.06	0.045	0.021	367
BR	0.931	1.99	1.22	0.137	0.364	0.03	0.05	0.032	0.016	412
ETR	0.950	1.71	1.02	0.109	0.258	0.02	0.04	0.023	0.014	302
GBM	0.887	2.42	1.47	0.184	0.501	0.06	0.08	0.056	0.018	532
ANNs	0.914	2.01	1.25	0.152	0.375	0.04	0.06	0.039	0.017	607
RNNs	0.941	1.72	1.05	0.12	0.269	0.02	0.05	0.028	0.015	677
Stacked ML	0.989	1.51	0.96	0.101	0.242	0.01	0.03	0.019	0.011	721

Table A-7
Results of error indicators for the ID distribution of the 8-Story BRBFs assuming the mean method.

ML algorithm	R^2	MSE	MAE	MARE	MSRE	RMSRE	MBE	erMAX	SD	Execution time (sec)
XGBoost	0.919	2.19	1.41	0.177	0.494	0.05	0.06	0.046	0.021	454
RF	0.903	2.27	1.32	0.167	0.481	0.05	0.06	0.045	0.021	421
BR	0.943	1.87	1.21	0.134	0.361	0.03	0.05	0.032	0.016	478
ETR	0.957	1.66	1.01	0.108	0.256	0.02	0.04	0.023	0.014	320
GBM	0.896	2.34	1.44	0.182	0.498	0.06	0.08	0.056	0.018	502
ANNs	0.936	1.97	1.23	0.15	0.370	0.04	0.06	0.039	0.017	514
RNNs	0.948	1.63	1.03	0.118	0.266	0.02	0.05	0.028	0.015	642
Stacked ML	0.965	1.45	0.94	0.099	0.238	0.01	0.03	0.028	0.012	787

Table A-8
Results of error indicators for the ID distribution of the 10-Story BRBFs assuming the median method.

ML algorithm	R^2	MSE	MAE	MARE	MSRE	RMSRE	MBE	erMAX	SD	Execution time (sec)
XGBoost	0.949	1.78	1.22	0.140	0.367	0.03	0.05	0.031	0.016	461
RF	0.919	2.25	1.38	0.169	0.421	0.04	0.06	0.041	0.018	367
BR	0.892	2.89	1.51	0.193	0.493	0.05	0.08	0.051	0.021	442
ETR	0.904	2.70	1.47	0.181	0.458	0.04	0.07	0.047	0.019	306
GBM	0.862	3.88	1.74	0.221	0.558	0.07	0.10	0.067	0.024	522
ANNs	0.896	3.12	1.65	0.207	0.514	0.06	0.09	0.057	0.022	595
RNNs	0.910	2.95	1.56	0.198	0.485	0.05	0.08	0.051	0.021	689
Stacked ML	0.977	1.85	1.18	0.142	0.371	0.03	0.06	0.032	0.017	763

Table A-9
Results of error indicators for the ID distribution of the 10-Story BRBFs assuming the mean method.

ML algorithm	R^2	MSE	MAE	MARE	MSRE	RMSRE	MBE	erMAX	SD	Execution time (sec)
XGBoost	0.943	2.03	1.31	0.154	0.389	0.03	0.05	0.035	0.017	509
RF	0.947	2.37	1.42	0.169	0.431	0.04	0.06	0.042	0.019	378
BR	0.931	2.90	1.53	0.187	0.475	0.05	0.08	0.049	0.022	415
ETR	0.950	2.65	1.35	0.163	0.414	0.04	0.07	0.038	0.018	299
GBM	0.890	4.10	1.85	0.217	0.530	0.06	0.09	0.062	0.024	521
ANNs	0.915	3.44	1.71	0.201	0.477	0.05	0.08	0.048	0.021	602
RNNs	0.938	2.92	1.48	0.179	0.428	0.04	0.06	0.042	0.019	679
Stacked ML	0.988	1.76	1.14	0.138	0.362	0.03	0.05	0.032	0.016	752

Table A-10
Results of error indicators for the ID distribution of the 12-Story BRBFs assuming the median method.

ML algorithm	R^2	MSE	MAE	MARE	MSRE	RMSRE	MBE	erMAX	SD	Execution time (sec)
XGBoost	0.958	1.65	1.16	0.129	0.314	0.02	0.04	0.027	0.015	488
RF	0.937	2.46	1.37	0.165	0.414	0.04	0.06	0.042	0.019	421
BR	0.932	2.65	1.47	0.179	0.464	0.05	0.07	0.046	0.021	403
ETR	0.948	2.38	1.29	0.153	0.375	0.03	0.05	0.033	0.017	328
GBM	0.908	3.18	1.72	0.202	0.495	0.06	0.08	0.054	0.022	502
ANNs	0.925	2.80	1.56	0.188	0.449	0.04	0.07	0.044	0.022	612
RNNs	0.939	2.55	1.45	0.175	0.407	0.04	0.06	0.038	0.018	709
Stacked ML	0.988	1.59	1.08	0.121	0.296	0.02	0.04	0.025	0.015	825

Table A-11
Results of error indicators for the ID distribution of the 12-Story BRBFs assuming the mean method.

ML algorithm	R^2	MSE	MAE	MARE	MSRE	RMSRE	MBE	erMAX	SD	Execution time (sec)
XGBoost	0.946	1.72	1.18	0.132	0.324	0.02	0.04	0.027	0.015	480
RF	0.944	2.52	1.39	0.166	0.412	0.04	0.06	0.04	0.019	377
BR	0.928	2.82	1.55	0.180	0.462	0.05	0.07	0.046	0.021	402
ETR	0.942	2.61	1.34	0.152	0.374	0.03	0.05	0.033	0.017	315
GBM	0.906	3.29	1.77	0.204	0.502	0.05	0.08	0.053	0.022	521
ANNs	0.921	2.92	1.60	0.186	0.445	0.04	0.07	0.044	0.02	594
RNNs	0.934	2.68	1.43	0.172	0.407	0.04	0.06	0.038	0.018	659
Stacked ML	0.989	1.63	1.09	0.120	0.297	0.02	0.04	0.026	0.015	792

Table A-12
Results of error indicators for the RID distribution of the 2-Story BRBFs assuming the median method.

ML algorithm	R^2	MSE	MAE	MARE	MSRE	RMSRE	MBE	erMAX	SD	Execution time (sec)
XGBoost	0.901	2.85	1.47	0.55	0.613	0.05	0.14	0.06	0.04	482
RF	0.900	2.81	1.44	0.53	0.610	0.05	0.13	0.05	0.04	542
BR	0.905	2.67	1.35	0.49	0.605	0.05	0.12	0.04	0.03	441
ETR	0.898	2.89	1.49	0.56	0.616	0.06	0.15	0.06	0.05	369
GBM	0.899	2.83	1.46	0.54	0.612	0.05	0.14	0.05	0.04	523
ANNs	0.906	2.64	1.32	0.47	0.604	0.05	0.11	0.04	0.03	602
RNNs	0.902	2.78	1.42	0.52	0.609	0.05	0.13	0.05	0.04	678
Stacked ML	0.978	1.38	1.09	0.21	0.569	0.04	0.08	0.03	0.02	812

Table A-13
Results of error indicators for the RID distribution of the 2-Story BRBFs assuming the mean method.

ML algorithm	R^2	MSE	MAE	MARE	MSRE	RMSRE	MBE	erMAX	SD	Execution time (sec)
XGBoost	0.899	3.12	1.45	0.55	0.615	0.05	0.14	0.06	0.031	502
RF	0.898	3.21	1.54	0.62	0.622	0.06	0.17	0.07	0.029	385
BR	0.882	3.56	1.51	0.59	0.637	0.07	0.15	0.08	0.028	443
ETR	0.875	3.76	1.62	0.64	0.645	0.08	0.19	0.09	0.027	321
GBM	0.913	2.88	1.35	0.51	0.612	0.05	0.13	0.05	0.03	564
ANNs	0.924	2.74	1.33	0.50	0.608	0.04	0.12	0.05	0.032	642
RNNs	0.913	2.89	1.34	0.53	0.615	0.05	0.14	0.06	0.031	715
Stacked ML	0.985	1.15	1.05	0.35	0.550	0.03	0.08	0.04	0.023	803

Table A-14
Results of error indicators for the RID distribution of the 4-Story BRBFs assuming the median method.

ML algorithm	R^2	MSE	MAE	MARE	MSRE	RMSRE	MBE	erMAX	SD	Execution time (sec)
XGBoost	0.913	2.55	1.25	0.45	0.593	0.04	0.12	0.05	0.03	450
RF	0.930	3.39	1.50	0.69	0.634	0.07	0.17	0.07	0.03	391
BR	0.921	3.02	1.36	0.48	0.601	0.04	0.11	0.05	0.02	419
ETR	0.942	2.21	1.18	0.36	0.579	0.03	0.08	0.04	0.02	344
GBM	0.903	3.67	1.60	0.75	0.645	0.06	0.19	0.06	0.03	511
ANNs	0.889	3.82	1.68	0.72	0.660	0.05	0.21	0.07	0.03	608
RNNs	0.878	3.99	1.74	0.65	0.678	0.05	0.24	0.08	0.04	702
Stacked ML	0.989	1.25	0.95	0.22	0.550	0.03	0.06	0.02	0.01	783

Table A-15
Results of error indicators for the RID distribution of the 4-Story BRBFs assuming the mean method.

ML algorithm	R^2	MSE	MAE	MARE	MSRE	RMSRE	MBE	erMAX	SD	Execution time (sec)
XGBoost	0.888	2.44	1.22	0.45	0.580	0.04	0.12	0.048	0.029	472
RF	0.891	3.11	1.33	0.61	0.607	0.07	0.17	0.066	0.032	560
BR	0.875	2.21	1.13	0.37	0.570	0.04	0.08	0.037	0.021	428
ETR	0.916	1.97	1.06	0.29	0.550	0.03	0.07	0.034	0.019	318
GBM	0.896	2.78	1.27	0.47	0.590	0.05	0.14	0.054	0.027	536
ANNs	0.905	2.36	1.18	0.43	0.574	0.04	0.11	0.043	0.025	564
RNNs	0.911	2.05	1.12	0.39	0.562	0.04	0.09	0.036	0.022	673
Stacked ML	0.978	1.21	1.02	0.21	0.498	0.03	0.08	0.031	0.021	745

Table A-16
Results of error indicators for the RID distribution of the 8-Story BRBFs assuming the median method.

ML algorithm	R^2	MSE	MAE	MARE	MSRE	RMSRE	MBE	erMAX	SD	Execution time (sec)
XGBoost	0.910	2.40	1.25	0.47	0.591	0.04	0.11	0.047	0.031	460
RF	0.889	3.20	1.38	0.62	0.608	0.07	0.18	0.067	0.033	388
BR	0.879	2.19	1.10	0.38	0.570	0.04	0.08	0.036	0.021	413
ETR	0.935	1.97	1.08	0.32	0.552	0.04	0.07	0.035	0.02	330
GBM	0.907	2.80	1.29	0.48	0.592	0.05	0.14	0.054	0.027	502
ANNs	0.925	2.42	1.21	0.44	0.575	0.04	0.11	0.042	0.025	611
RNNs	0.930	2.06	1.13	0.41	0.562	0.04	0.09	0.037	0.022	675
Stacked ML	0.981	1.34	1.03	0.31	0.543	0.03	0.09	0.034	0.017	834

Table A-17
Results of error indicators for the RID distribution of the 8-Story BRBFs assuming the mean method.

ML algorithm	R^2	MSE	MAE	MARE	MSRE	RMSRE	MBE	erMAX	SD	Execution time (sec)
XGBoost	0.932	2.50	1.26	0.48	0.595	0.04	0.11	0.046	0.031	450
RF	0.912	3.30	1.42	0.65	0.613	0.07	0.19	0.068	0.034	399
BR	0.888	2.26	1.11	0.38	0.572	0.04	0.08	0.036	0.022	365
ETR	0.942	1.95	1.07	0.30	0.549	0.04	0.07	0.035	0.020	308
GBM	0.920	2.75	1.28	0.47	0.589	0.05	0.14	0.054	0.026	502
ANNs	0.938	2.38	1.23	0.43	0.574	0.04	0.11	0.042	0.025	568
RNNs	0.945	2.05	1.13	0.39	0.562	0.04	0.09	0.037	0.022	633
Stacked ML	0.972	1.41	1.12	0.24	0.571	0.03	0.09	0.043	0.018	845

Table A-18
Results of error indicators for the RID distribution of the 10-Story BRBFs assuming the median method.

ML algorithm	R^2	MSE	MAE	MARE	MSRE	RMSRE	MBE	erMAX	SD	Execution time (sec)
XGBoost	0.915	2.46	1.24	0.46	0.588	0.04	0.11	0.047	0.03	472
RF	0.900	3.15	1.36	0.62	0.607	0.07	0.18	0.067	0.033	359
BR	0.882	2.20	1.10	0.38	0.570	0.04	0.08	0.036	0.021	413
ETR	0.930	1.98	1.08	0.30	0.553	0.04	0.07	0.035	0.020	306
GBM	0.910	2.76	1.29	0.48	0.592	0.05	0.14	0.054	0.027	521
ANNs	0.930	2.43	1.21	0.44	0.575	0.04	0.11	0.042	0.025	589
RNNs	0.937	2.04	1.12	0.39	0.561	0.04	0.09	0.037	0.022	677
Stacked ML	0.983	1.47	1.07	0.24	0.565	0.03	0.09	0.040	0.021	796

Table A-19
Results of error indicators for the RID distribution of the 10-Story BRBFs assuming the mean method.

ML algorithm	R^2	MSE	MAE	MARE	MSRE	RMSRE	MBE	erMAX	SD	Execution time (sec)
XGBoost	0.943	2.34	1.18	0.45	0.583	0.04	0.11	0.047	0.031	523
RF	0.917	3.05	1.32	0.59	0.605	0.07	0.17	0.065	0.032	411
BR	0.898	2.17	1.09	0.36	0.569	0.04	0.08	0.036	0.02	388
ETR	0.967	1.92	1.04	0.28	0.545	0.03	0.07	0.033	0.019	290
GBM	0.926	2.65	1.23	0.46	0.590	0.05	0.14	0.053	0.027	589
ANNs	0.937	2.32	1.17	0.42	0.573	0.04	0.11	0.042	0.025	634
RNNs	0.952	1.99	1.10	0.38	0.557	0.04	0.09	0.035	0.022	698
Stacked ML	0.980	1.34	1.08	0.23	0.520	0.03	0.08	0.038	0.023	911

Table A-20
Results of error indicators for the RID distribution of the 12-Story BRBFs assuming the median method.

ML algorithm	R^2	MSE	MAE	MARE	MSRE	RMSRE	MBE	erMAX	SD	Execution time (sec)
XGBoost	0.956	2.22	1.14	0.44	0.577	0.04	0.11	0.047	0.031	478
RF	0.912	3.25	1.36	0.61	0.610	0.07	0.18	0.065	0.032	367
BR	0.885	2.13	1.07	0.36	0.568	0.04	0.08	0.036	0.020	413
ETR	0.973	1.89	1.03	0.28	0.544	0.03	0.07	0.033	0.019	297
GBM	0.934	2.55	1.21	0.46	0.589	0.05	0.14	0.053	0.027	523
ANNs	0.943	2.26	1.16	0.42	0.572	0.04	0.11	0.042	0.025	605
RNNs	0.957	1.95	1.08	0.38	0.556	0.04	0.09	0.035	0.022	678
Stacked ML	0.988	1.39	1.09	0.23	0.569	0.03	0.09	0.041	0.022	822

Table A-21
Results of error indicators for the RID distribution of the 12-Story BRBFs assuming the mean method.

ML algorithm	R^2	MSE	MAE	MARE	MSRE	RMSRE	MBE	erMAX	SD	Execution time (sec)
XGBoost	0.967	2.15	1.14	0.43	0.574	0.04	0.11	0.047	0.03	495
RF	0.925	3.18	1.33	0.62	0.608	0.07	0.17	0.065	0.032	371
BR	0.892	2.15	1.08	0.37	0.569	0.04	0.08	0.036	0.02	427
ETR	0.963	1.88	1.02	0.27	0.543	0.03	0.07	0.033	0.019	319
GBM	0.942	2.54	1.19	0.45	0.587	0.05	0.14	0.053	0.027	569
ANNs	0.951	2.28	1.14	0.41	0.570	0.04	0.11	0.042	0.025	625
RNNs	0.962	1.93	1.06	0.37	0.555	0.04	0.09	0.035	0.022	688
Stacked ML	0.976	1.38	1.08	0.24	0.564	0.03	0.09	0.037	0.018	714

References

AISC 341-16, 2016. Seismic Provisions for Structural Steel Buildings. American Institute of Steel Construction, Chicago, IL.

ANSI/AISC 360– 16, 2016. Specification for Structural Steel Buildings. American Institute of Steel Construction, Chicago-Illinois.

ASCE/SEI 7-16, 2017. Minimum Design Loads for Buildings and Other Structures. American Society of Civil Engineers, Reston, VA.

Asgarkhani, N., Yakhchalian, M., Mohebi, B., 2020. Evaluation of approximate methods for estimating residual drift demands in BRBFs. Eng. Struct. 224, 110849.

Asgarkhani, N., Kazemi, F., Jankowski, R., 2023. Machine Learning-Based Prediction of Residual Drift and Seismic Risk Assessment of Steel Moment-Resisting Frames Considering Soil-Structure Interaction. Compu. & Struct. 289, 107181.

Baiguera, M., Vasdravellis, G., Karavasilis, T.L., 2016. Dual seismic-resistant steel frame with high post-yield stiffness energy-dissipative braces for residual drift reduction. J. Constr. Steel Res. 122, 198–212.

Barbagallo, F., Bosco, M., Marino, E.M., Rossi, P.P., 2019. Achieving a more effective concentric braced frame by the double-stage yield BRB. Eng. Struct. 186, 484–497.

Cole, G.L., Dhakal, R.P., Turner, F.M., 2012. Building pounding damage observed in the 2011 Christchurch earthquake. Earthq. Eng. Struct. Dynam. 41 (5), 893–913.

Deylami, A., Mahdavipour, M.A., 2016. Probabilistic seismic demand assessment of residual drift for Buckling-Restrained Braced Frames as a dual system. Struct. Saf. 58, 31–39.

Erochko, J., Christopoulos, C., Tremblay, R., Choi, H., 2011. Residual drift response of SMRFs and BRB frames in steel buildings designed according to ASCE 7-05. J. Struct. Eng. 137 (5), 589–599.

FEMA P-58, 2012. Seismic Performance Assessment of Buildings Volume 1 – Methodology. Federal Emergency Management Agency, Washington DC.

Feng, D.C., Wang, W.J., Mangalathu, S., Hu, G., Wu, T., 2021. Implementing ensemble learning methods to predict the shear strength of RC deep beams with/without web reinforcements. Eng. Struct. 235, 111979.

Friedman, J.H., 2001. Greedy function approximation: a gradient boosting machine. Ann. Stat. 1189–1232.

GCR 10-917-8, 2010. Evaluation of the FEMA P-695 Methodology for Quantification of Building Seismic Performance Factors. National Institute of Standards and Technology (NIST).

Gholami, M., Zare, E., Azandariani, M.G., Moradifard, R., 2021. Seismic behavior of dual buckling-restrained steel braced frame with eccentric configuration and post-tensioned frame system. Soil Dynam. Earthq. Eng. 151, 106977.

Ghowsi, A.F., Sahoo, D.R., 2020. Seismic response of SMA-based self-centering buckling-restrained braced frames under near-fault ground motions. Soil Dynam. Earthq. Eng. 139, 106397.

Giugliano, M.T., Longo, A., Montuori, R., Piluso, V., 2010. Plastic design of CB-frames with reduced section solution for bracing members. J. Constr. Steel Res. 66 (5), 611–621.

Guerrero, H., Ji, T., Teran-Gilmore, A., Escobar, J.A., 2016. A method for preliminary seismic design and assessment of low-rise structures protected with buckling-restrained braces. Eng. Struct. 123, 141–154.

Haselton, C.B., 2006. Assessing Collapse Safety of Modern Reinforced Concrete Moment Frame Buildings. Department of Civil and Environmental Engineering, Stanford University, Stanford, CA. PhD dissertation.

Haselton, C.B., Deierlein, G.G., 2007. Assessing seismic collapse safety of modern reinforced concrete frame buildings. PEER report 8.

Jagruthi, N., Sharathchandran, K., Pandikkadavath, M.S., Mangalathu, S., Reddy, K.M., Nair, A., Sahoo, D.R., 2022. Machine learning-based seismic drift response estimation of buckling-restrained braced frames. In: Symposium in Earthquake Engineering. Springer Nature Singapore, Singapore, pp. 837–848.

Jia, L.J., Ge, H., Maruyama, R., Shinohara, K., 2017. Development of a novel high-performance all-steel fish-bone shaped buckling-restrained brace. Eng. Struct. 138, 105–119.

Kazemi, F., Jankowski, R., 2023. Machine learning-based prediction of seismic limit-state capacity of steel moment-resisting frames considering soil-structure interaction. Comput. Struct. 274, 106886.

Kazemi, F., Asgarkhani, N., Jankowski, R., 2023a. Machine learning-based seismic fragility and seismic vulnerability assessment of reinforced concrete structures. Soil Dynam. Earthq. Eng. 166, 107761.

Kazemi, F., Asgarkhani, N., Jankowski, R., 2023b. Predicting seismic response of SMRFs founded on different soil types using machine learning techniques. Eng. Struct. 274, 114953.

Kazemi, F., Asgarkhani, N., Jankowski, R., 2023c. Machine learning-based seismic response and performance assessment of reinforced concrete buildings. Arch. Civ. Mech. Eng. 23 (2), 94.

Kiani, J., Camp, C., Pezeshk, S., 2019. On the application of machine learning techniques to derive seismic fragility curves. Comput. Struct. 218, 108–122, 290.

Maley, T.J., Sullivan, T.J., Corte, G.D., 2010. Development of a displacement-based design method for steel dual systems with buckling-restrained braces and moment-resisting frames. J. Earthq. Eng. 14 (S1), 106–140.

Mazzoni, S., McKenna, F., Scott, M.H., Fenves, G.L., 2006. OpenSees Command Language Manual. Pacific Earthquake Engineering Research Center, Berkeley, CA.

McCormick, J., Aburano, H., Ikenaga, M., Nakashima, M., 2008. Permissible residual deformation levels for building structures considering both safety and human elements. In: Proceedings of the 14th World Conference on Earthquake Engineering. Seismological Press Beijing, pp. 12–17.

McKenna, F., Fenves, G.L., Scott, M.H., 2015. Open System for Earthquake Engineering Simulation. Pacific Earthquake Engineering Research Center, Berkeley, CA.

Meng, Z., Qian, Q., Xu, M., Yu, B., Yıldız, A.R., Mirjalili, S., 2023. PINN-FORM: a new physics-informed neural network for reliability analysis with partial differential equation. Comput. Methods Appl. Mech. Eng. 414, 116172.

Montuori, R., Nastri, E., Piluso, V., 2016. Theory of plastic mechanism control for MRF–EBF dual systems: closed form solution. Eng. Struct. 118, 287–306.

Oh, B.K., Glisic, B., Park, S.W., Park, H.S., 2020. Neural network-based seismic response prediction model for building structures using artificial earthquakes. J. Sound Vib. 468, 115109.

Panagant, N., Pholdee, N., Bureerat, S., Yildiz, A.R., Mirjalili, S., 2021. A comparative study of recent multi-objective metaheuristics for solving constrained truss optimisation problems. Arch. Comput. Methods Eng. 1–17.

Ruiz-García, J., Chora, C., 2015. Evaluation of approximate methods to estimate residual drift demands in steel framed buildings. Earthq. Eng. Struct. Dynam. 44 (15), 2837–2854.

Ruiz-Garcia, J., Miranda, E., 2010. Probabilistic estimation of residual drift demands for seismic assessment of multi-story framed buildings. Eng. Struct. 32 (1), 11–20.

Sabelli, R., Mahin, S., Chang, C., 2003. Seismic demands on steel braced frame buildings with buckling-restrained braces. Eng. Struct. 25 (5), 655–666.

Shafighfard, T., Bagherzadeh, F., Rizi, R.A., Yoo, D.Y., 2022a. Data-driven compressive strength prediction of steel fiber reinforced concrete (SFRC) subjected to elevated temperatures using stacked machine learning algorithms. J. Mater. Res. Technol. 21, 3777–3794.

Sun, B., Zhang, Y., Huang, C., 2020. Machine learning-based seismic fragility analysis of large-scale steel buckling restrained brace frames. CMES-Computer Modeling in Engineering & Sciences 125 (2).

Tamimi, M.F., Alshannaq, A.A., Mu'ath, I., 2023. Sensitivity and reliability assessment of buckling restrained braces using machine learning assisted-simulation. J. Constr. Steel Res. 211, 108187.

Todorov, B., Billah, A.M., 2022. Machine learning driven seismic performance limit state identification for performance-based seismic design of bridge piers. Eng. Struct. 255, 113919.

Xie, Q., Zhou, Z., Meng, S.P., 2020. Experimental investigation of the hysteretic performance of self-centering buckling-restrained braces with friction fuses. Eng. Struct. 203, 109865.

Yahyazadeh, A., Yakhchalian, M., 2020. Probabilistic evaluation of residual drift demands in steel moment resisting frames equipped with linear and nonlinear fluid viscous dampers. Bull. Earth. Sci. Eng. 7 (3), 97–113.

Yakhchalian, M., Asgarkhani, N., Yakhchalian, M., 2020. Evaluation of deflection amplification factor for steel buckling restrained braced frames. J. Build. Eng. 30, 101228.

Yakhchalian, M., Yakhchalian, M., Asgarkhani, N., 2021. An advanced intensity measure for residual drift assessment of steel BRB frames. Bull. Earthq. Eng. 19, 1931–1955.

Zhang, Y., Burton, H.V., 2019. Pattern recognition approach to assess the residual structural capacity of damaged tall buildings. Struct. Saf. 78, 12–22.